Poultry Science®

Online chicken carcass volume estimation using depth imaging and 3-D reconstruction

Innocent Nyalala ,*,† Zhang Jiayu,* Chen Zixuan,‡ Chen Junlong,‡ and Kunjie Chen*,1

*College of Engineering, Nanjing Agricultural University, Nanjing, Jiangsu, 210031, China; †Faculty of Science, Department of Computer Science, Egerton University, Njoro, Kenya; and ‡Nanjing Institute of Agricultural Mechanization, Ministry of Agriculture and Rural Affairs, Nanjing, Jiangsu, 210014, China

ABSTRACT Variability in the size of slaughtered chickens remains a longstanding challenge in the standardization of the poultry industry. To address this issue, we present a novel approach that uses volume as a grading metric for chicken carcasses. This innovative method, unexplored in existing studies, employs real-time data capture of moving chicken carcasses on a production line using Kinect v2 depth imaging and 3-D reconstruction technologies. The captured depth images are processed into point clouds followed by 3-D reconstruction. Volume is calculated from the reconstructed models using the surface integration method, and additional 2-D and 3-D features are extracted as input parameters for machine learning models. Multiple regression models were evaluated, with the bagged tree model demonstrating superior performance, achieving an R^2 value of 0.9988, RMSE of 5.335, and ARE of 2.125%. Furthermore, our method showed remarkable efficiency with an average processing time of less than 1.6 seconds per carcass. These results indicate that our novel approach fills a critical gap in existing automated grading methodologies by offering both accuracy and efficiency. This validates the applicability of depth imaging, 3-D reconstruction, and machine learning for estimating chicken carcass volume with high precision, thereby enabling a more comprehensive, efficient, and reliable chicken carcass grading system.

Key words: chicken carcass, depth imaging, 3-D reconstruction, poultry grading, volume estimation

2024 Poultry Science 103:104232
https://doi.org/10.1016/j.psj.2024.104232

INTRODUCTION

Rapid growth in global food demand has significantly impacted the poultry sector, which has expanded from 13.90 billion broilers in 2000 to 25.85 billion in 2021. The global poultry industry has witnessed a substantial increase in consumption, projected to surpass pork as the most consumed meat by 2032, with an expected demand of 156.24 metric kilotons (Shahbandeh, 2023). This accelerated growth necessitates the development of effective poultry grading systems that can handle increased production volumes, while ensuring quality and consistency. Efficient grading is crucial not only for maintaining product quality, but also for optimizing supply chain operations and reducing economic losses due to inaccurate assessments (Nyalala, et al., 2021b). Traditional grading methods, which are often manual and subjective, are insufficient for meeting the industry's current demands. Therefore, there is an urgent need for advanced automated grading systems that provide accurate and consistent results.

Existing systems rely mainly on manual or semi-automated methods, which are error-prone and economically unsustainable (Mortensen, et al., 2016). Inaccurate measurements can lead to considerable waste and compromise the product quality. For instance, oversized carcasses may result in suboptimal meat cuts, whereas undersized carcasses may contain bones and ribs, which adversely affects waste and profitability (Jørgensen et al., 2019). These issues are magnified by the high volume and low margin characteristics of the poultry industry.

Despite the implementation of automated systems, traditional grading methods struggle with variability in muscle proportions across carcasses (Adamczak, et al., 2018). These methods, which often rely on 2-D imaging, fail to capture the true volumetric characteristics of carcasses owing to occlusions and manual handling errors, leading to inaccuracies in volume estimation. High-cost and invasive techniques, such as MRI and ultrasound, are impractical for routine use in the industry (Scollan et al., 1998; Oviedo-Rondon, et al., 2007). Advances in

Received April 16, 2024.
Accepted August 13, 2024.

[1]Corresponding author: kunjiechen@njau.edu.cn

computer vision and machine learning have shown promise, but existing approaches are mostly limited to 2-D imaging, which overlooks the complex spatial features of chicken carcasses (Nyalala, et al., 2021c).

Recently, Jørgensen et al. improved upon this by using 3-D features for weight estimation; however, their study did not explore volume as a primary grading metric (Jørgensen et al., 2019). Previous studies have primarily focused on weight as a metric for poultry grading, overlooking volumetric characteristics that could provide a more comprehensive understanding of carcass quality (Nyalala et al., 2021b,c). Therefore, there is an urgent need for innovative, dependable, and economically viable grading systems that provide automated, noncontact, and accurate volume measurements. To address this need, researchers have explored various technological solutions, such as image analysis and machine learning algorithms, to develop such grading systems. Our proposed method using Kinect v2 and 3-D reconstruction aims to overcome these limitations by capturing comprehensive spatial data, thereby improving the accuracy and efficiency of the grading process. By leveraging advanced 3-D reconstruction techniques and the precision offered by Kinect v2, our proposed method promises to significantly enhance the accuracy and speed of the grading process, thereby empowering instructors to make more informed decisions.

Automation is essential; however, its integration into existing production systems presents challenges owing to operational disruptions and financial limitations (Okinda et al., 2020b). This study proposes a new grading methodology that utilizes 3-D reconstruction along with machine learning to determine the volume of chicken carcasses. This approach takes advantage of 2-D and 3-D features derived from depth images captured using Microsoft Kinect v2. By combining these two methods, the accuracy, efficiency, and cost-effectiveness of the grading system can be improved significantly. The depth images and 3-D reconstruction provided a comprehensive view of the chicken carcasses, allowing for a more thorough and precise grading process.

The primary objective of this study was to develop and validate a novel technique for estimating the volume of chicken carcasses using Kinect v2 depth imaging and 3-D reconstruction technology. To the best of our knowledge, this study represents the first attempt to provide a solution for estimating the chicken carcass volume. To achieve this, the specific objectives include: 1) designing a real-time data capture system with Kinect v2 for moving chicken carcasses on a production line; 2) transforming depth images into point clouds and executing a 3-D reconstruction; 3) utilizing the surface integration method to calculate the volume of the reconstructed models; 4) extracting relevant 2-D and 3-D features for machine learning applications; 5) evaluating multiple regression models to identify the optimal predictor of carcass volume; and 6) ensuring the real-time efficiency of our methodology.

This study introduces an innovative real-time volume estimation method that leverages the synergy between depth imaging and advanced machine learning algorithms, offering a noninvasive, efficient, and scalable solution.

MATERIALS AND METHODS

Chicken Carcass Samples

Chicken carcasses were obtained from Nanjing Sushi Meat Products Co. Ltd. in Pukou District, Nanjing, China, to ensure a comprehensive representation of the poultry industry, including a variety of sizes, species, and conditions commonly encountered in real-world poultry production. Uniformity of the dataset is essential for meaningful analysis, and we achieved this through a careful selection process that minimized potential variations that could introduce bias or uncertainty into the subsequent data acquisition and analysis. This precautionary measure also ensured that the carcasses were free from visible injuries, defects, and signs of frost, which was a critical step in preventing potential anomalies in data acquisition. By establishing a solid framework using carefully selected and uniformly prepared chicken carcass samples, we were able to collect and analyze reliable and insightful data.

Kinect v2 Sensor: Hardware Setup and Calibration

The Kinect v2 sensor, a device that captures the shape and size of objects in three dimensions, was used to create digital models of the chicken carcasses for analysis. We selected the Kinect v2 depth camera because of its superior resolution, wide field of view, and enhanced depth accuracy compared with other commercially available depth cameras (Yang, et al., 2015). Its cost-effectiveness and widespread availability make it suitable for practical application in poultry processing plants. The Kinect v2 sensor was strategically positioned to ensure comprehensive coverage and capture the detailed spatial dimensions of the chicken carcasses from various angles. The acquisition environment and hardware setup are shown in Figure 1.

We adjusted the camera settings to maintain the carcasses at the central focal point to ensure high-quality images and accurately determine the intricate details of moving chicken carcasses at a speed of 0.5 meters per second on the production line; we carefully adjusted the camera settings to maintain the carcasses at the central focal point. We used a frame rate of 30 fps and employed multiple viewpoints to create a comprehensive visual dataset encompassing the entire range of chicken carcasses. Depth images were generated using multi-angle imaging, leaving no carcass aspects unexamined.

To provide a comprehensive representation, the dataset consisted of 50 chicken carcasses, each of which was imaged from multiple angles, specifically approximately ± 30°. A total of 2,500 images were obtained and used for the training and validation of the regression models.

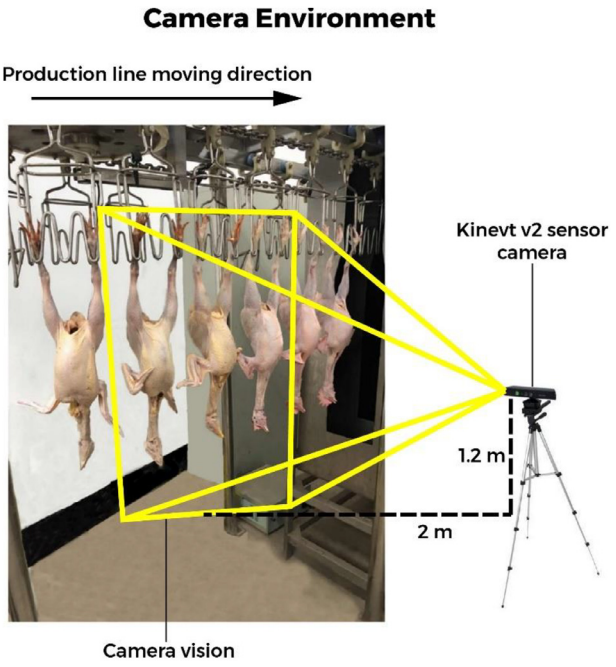

Figure 1. Detailed view of the acquisition environment and setup.

An example of the image acquisition process is shown in Figure 2. Table 1 provides detailed statistical information about the dataset.

The calibration process of the Kinect v2 sensor (Microsoft, Redmond) was essential to ensure the accuracy and reliability of the subsequent depth measurements. We adapted the calibration procedures reported by Lachat et al. (2015) and Pagliari and Pinto (2015) to map the objects of interest in images captured by the camera onto a universal world coordinate system. A standard checkerboard pattern with an 8 × 9 grid was used as the calibration target, allowing crucial calibration points to be extracted from the images captured at varying angles to accurately estimate the necessary intrinsic camera parameters.

The MATLAB calibration toolbox was employed with the default configuration (Pagliari and Pinto, 2015), excluding skew and tangential distortions and using only two radial distortion coefficients (K1 and K2). This method is suitable because it effectively corrects lens distortions and aligns depth images with RGB images, thereby ensuring precise depth measurements. The integration of MATLAB facilitated a streamlined calibration process, yielding essential intrinsic parameters, such as the focal length, principal point, and distortion coefficients. These parameters (Table 2) are vital for mitigating optical distortions, ensuring precise depth measurements, and laying the groundwork for accurate 3-D reconstruction and volume estimations.

By directly integrating the distortion coefficients into our point-cloud computation algorithm, we acquired a calibrated three-dimensional dataset, eliminated actual distortions in the initial depth map (Lachat et al., 2015). This comprehensive calibration ensures the reliability of the 3-D reconstruction and the accuracy of the volume estimation process, which is crucial for the effectiveness of our proposed grading system.

Carcass Detection Conditions

A critical aspect of computer vision systems for chicken carcass detection in poultry processing lines is defining depth-range criteria. This criterion restricts the detection of objects to a specific depth interval corresponding to the expected dimensions of the chicken carcasses. In this study, a depth range of 0.2 to 0.6 meters was selected to optimize the accuracy of the depth data for specific features of chicken carcasses. This range was chosen based on the specifications of the sensor and the need to minimize the influence of extraneous factors, such as background noise or other irrelevant objects on the production line (Wasenmüller and Stricker, 2017; Kurillo, et al., 2022). A size threshold of 500 square pixels was established to filter irrelevant objects and noise. This threshold ensured that only significant regions indicative of the carcass were processed for volume estimation. This is critical for maintaining computational efficiency and focusing on the analysis of the most relevant data points and regions for carcass estimation. This threshold eliminated the inclusion of insignificant artifacts in the analysis. Aspect ratio thresholds enhance detection accuracy by complementing size constraints. A threshold of 1.5 ensured that detected objects adhered to the expected proportions of chicken carcasses. This simultaneous application of the size and aspect ratio

Figure 2. Chicken carcasses positioned on an online processing conveyor system for automated volume estimation (A) Frontal view showing the orientation and spacing optimized for 3-D imaging (B) Side view illustrating a different camera angle.

Table 1. Descriptive statistics of the dataset.

Total number (chicken carcass)	50
Total images	2,500
Maximum	1,760 cm^3
Minimum	860 cm^3
Median	1,268 cm^3
Mean	1,286.6 cm^3
Standard deviation	187.99 cm^3
Variance	35,340.24 cm^3
Range	900 cm^3

Table 2. Kinect camera intrinsic parameters obtained via calibration.

	RGB camera	IR/Depth camera
Resolution (pixels)	1,920 × 1,080	512 × 424
Sensor size (μm)	3.1	10
Focal length x-axis (mm)	3.2831	3.6513
Focal length y-axis (mm)	3.5801	3.9680
Principal point x (pixel)	964.912	263.852
Principal point y (pixel)	583.268	225.717
K1 of radial distortion	9.1793 × 10−5	9.6582 × 10−5
K2 of radial distortion	−7.4231 × 10−8	−1.8173 × 10−7

constraints minimizes the risk of false positives arising from irrelevant sources.

Depth transition analysis is crucial for accurately distinguishing carcass boundaries. The system can distinguish genuine carcasses from noise-induced fluctuations by analyzing the gradients of depth values. This analysis focused on coherent spatial gradients, allowing for accurate identification of carcass contours. Adaptive noise thresholding enhances the robustness of the system against sensor noise by dynamically adjusting the threshold based on the local depth variations. This mechanism enables the system to effectively distinguish genuine detections from noise artifacts. Dynamic thresholding also contributes to the resilience of the systems in challenging environments. The detection conditions were designed to accommodate the real-time dynamics of carcass processing on the production line regardless of the orientation of the chicken carcass. The adaptability factor enhances the practical utility of a system in real-world scenarios.

Establishing Ground-Truth Measurements

To guarantee the accuracy of our depth-based volume estimation, we compared it with ground-truth measurements. The volume of each chicken carcass was calculated using the water displacement method, which is known for its precision in irregularly shaped objects (Nyalala, et al., 2019). The analyzed dataset comprised 2,500 images corresponding to a total of 50 chicken carcasses. Carcass volumes ranged from a minimum of 860 cm^3 to a maximum of 1,760 cm^3. The median volume was 1268 cm^3, indicating a distribution that was symmetric about the mean volume of 1,286.6 cm^3. The standard deviation was calculated to be 187.99 cm^3, with a variance of 35,340.24 cm^3, denoting a moderate degree of variability in carcass sizes. The overall range of the dataset was 900 cm^3, delineating the extent of the variation in the measured volumes. Ground-truth measurements are crucial for training and evaluating supervised-learning algorithms. These physical measurements served as concrete references against which our depth-based estimates were rigorously validated.

Image Preprocessing

A thorough preprocessing strategy was implemented on 50 depth images from each chicken carcass to ensure reliability and accuracy. This preprocessing phase serves as a crucial step between raw data and meaningful analysis, strengthening the validity of our results. The preprocessing workflow is outlined as follows.

1. Initialization and File Loading: We began pre-processing by arranging the depth images in the "raw data" directory. We extracted the images from the primary cell, converted them to double precision, and ensured that the following steps were performed with accurate computations.
2. Background Segmentation: Background Segmentation is a crucial preprocessing step for distinguishing chicken carcasses from the rest of an image. A global depth thresholding technique was employed, where pixels below a predefined threshold were classified as objects, and the rest were labeled as the background (Sahu et al., 2018).
3. Noise Reduction via Morphological Opening: Images were denoised using a 3-pixel radius disc-shaped element using the morphological opening technique (Said et al., 2016). This process aims to eliminate noise, remove unnecessary particles, and enhance the images for further analysis.
4. Noise Reduction via Order Filtering: A 5th-order order-statistic filter was used to reduce noise and improve image quality by suppressing salt-and-pepper noise.
5. Hole Filling: Hole Filling ensured that the chicken carcass was continuous and void-free. It fills sporadic gaps and provides complete and intact representation.
6. Boundary Smoothing via Active Contours: Dynamic boundary refinement was achieved using the adaptive "active contour" strategy. The Chan-Vese approach (Chan and Vese, 2001) optimizes boundary delineation to match intrinsic image features.
7. Image Normalization and Saving: Preprocessing ended with image normalization, creating a unified visual scale. After normalization, the images were converted into 8-bit unsigned integer TIFF files for further analysis.

Figure 3 shows the systematic approach undertaken for depth image processing of chicken carcasses, showing each pivotal phase from initial capture to background subtraction, morphological operations, and normalization.

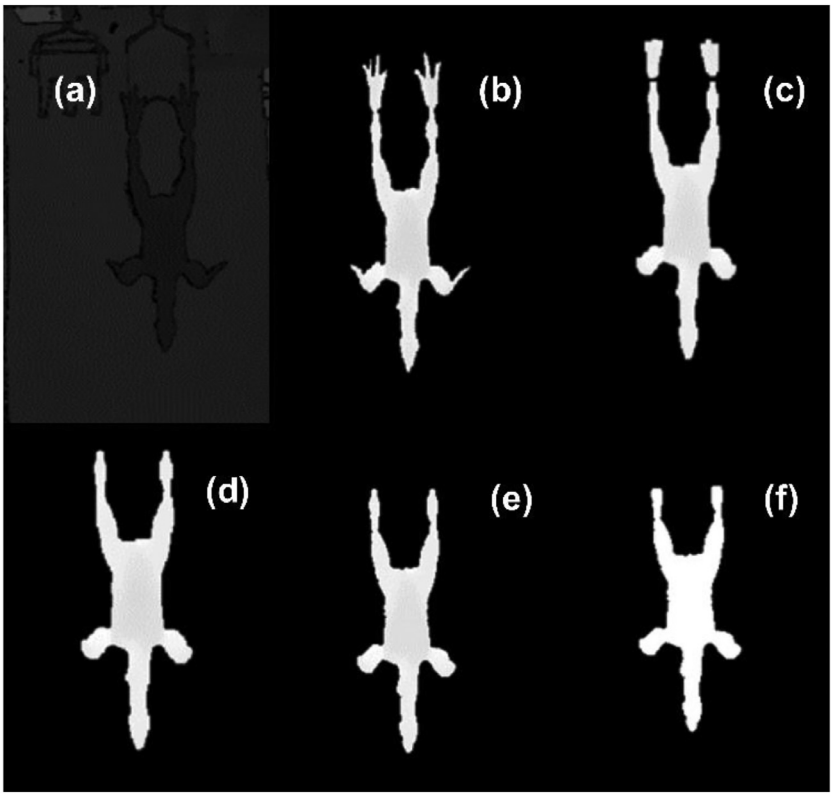

Figure 3. Sequential processing steps applied to the chicken carcass depth image: (A) initial depth image, (B) image following background subtraction, (C) image following morphological opening, (D) image subjected to order filtering, (E) image post-active contouring, and (F) image post-normalization.

This comprehensive preprocessing workflow highlights the importance of careful preparation of depth images for subsequent analysis, as the steps involved improve the image quality, enabling more refined analysis and reliable feature extraction. Figure 4 shows the raw depth images of the sample chicken carcasses, their resulting images after normalization, and the final processed image used for feature extraction.

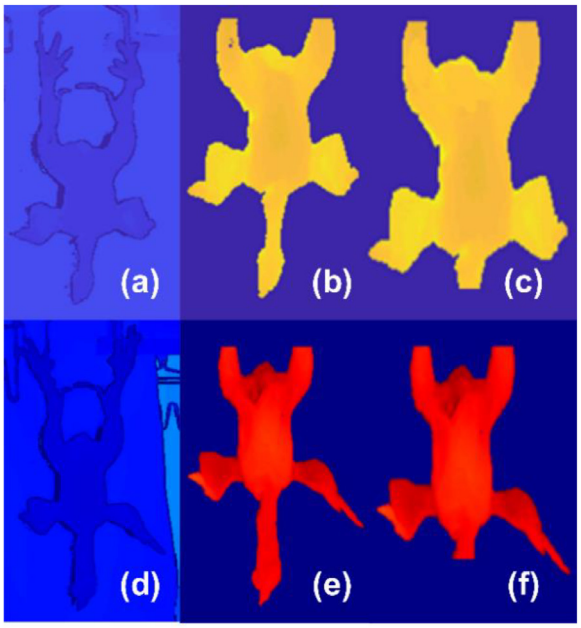

Figure 4. Depth image processing stages: (A), (D) original raw depth images (B), (E) normalized depth images, and (C), (F) final processed images for feature extraction.

Depth-to-Point Cloud Conversion

This section thoroughly examines the time-of-flight technology utilized by the Kinect v2 for depth sensing. Although effective, this technology is vulnerable to limitations such as noise and range constraints, which could compromise the accuracy of the depth measurements. To overcome these limitations, a comprehensive calibration process was performed. The focal length, lens distortion coefficients, and other intrinsic camera parameters were precisely estimated using optimization techniques, and their impact on depth measurement was evaluated using the root mean square error (**RMSE**) as an error metric (Pagliari and Pinto, 2015). The RMSE formula used for this evaluation was as follows:

$$\mathrm{RMSE} = \sqrt{\frac{1}{n}\sum_{i=1}^{n}\left(y_{\mathrm{obs},i} - y_{\mathrm{pred},i}\right)^2} \tag{1}$$

where $y_{\mathrm{obs},i}$ and $y_{\mathrm{pred},i}$ represent the observed and predicted depth values, respectively. The conversion of the depth values into a 3-D point cloud is mathematically grounded in geometric and trigonometric principles. Specifically, the depth value d at each pixel is converted into 3-D coordinates (X, Y, Z) using the following equation:

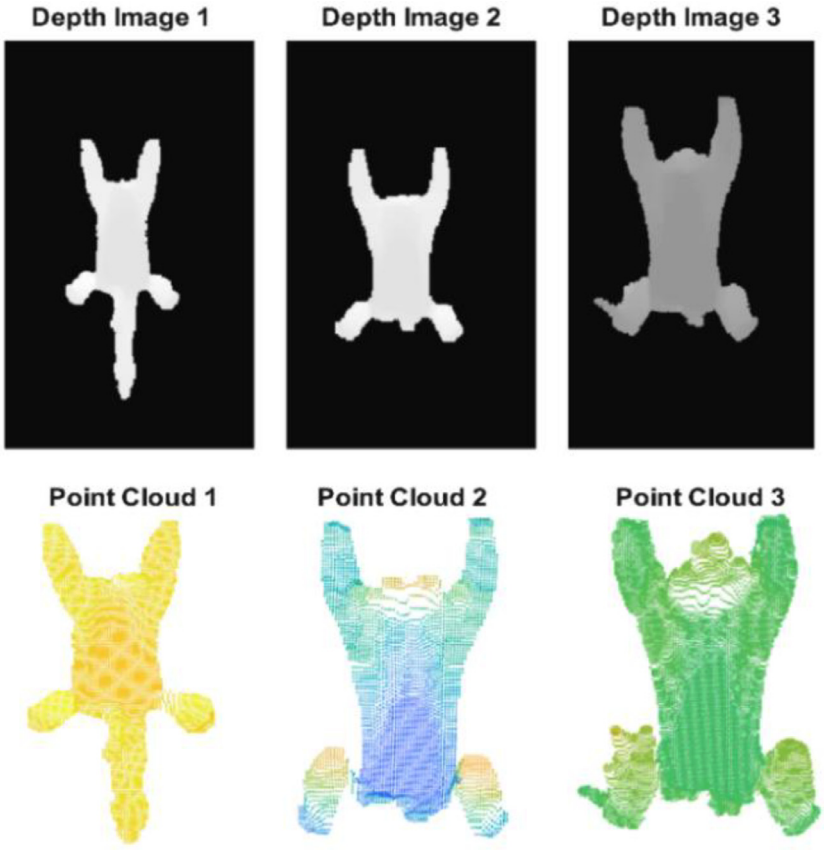

Figure 5. Chicken carcass point-cloud data representation.

$$(X, Y, Z) = \left(d \cdot \tan(\theta_x), d \cdot \tan\left(\theta_y\right), d\right) \quad (2)$$

where θ_x and θ_y are the angles relative to the optical axis (Hartley and Zisserman, 2003).

The accuracy of the transformation was heavily dependent on the camera parameters (Table 1). Intrinsic parameters were used to project depth values onto a 2-D image plane and real-world coordinates (Szeliski, 2022). No lens distortions were corrected using polynomial models derived from the calibration process. The accuracy and reliability of depth-to-point cloud conversion are crucial for achieving the research objectives, which focus on the precise 3-D reconstruction and volume estimation of chicken carcasses (Fig. 5). This process is critical for subsequent processes such as point cloud alignment and surface reconstruction.

Point Cloud Registration and Alignment

This section explores the crucial techniques of point cloud registration and alignment that are critical for building dependable 3-D models. We used the Iterative Closest Point (**ICP**) algorithm as the foundation of our alignment strategy (Holz, et al., 2015). Its variants, specifically point-to-plane and plane-to-plane ICP, have been emphasized because of their ability to effectively handle a range of surface geometries. Given the intricate structure of chicken carcasses, their versatility is essential.

The core mechanism of the ICP algorithm is iterative refinement, which aims to minimize the distance between corresponding points in disparate point clouds (Holz et al., 2015). Through this iterative process, we achieved an optimal alignment and captured subtle geometrical details, resulting in a unified point cloud that authentically represented the chicken carcass. This enhances the robustness and precision of the volume estimations.

Surface Mesh Reconstruction

This section explains the transformation of raw point clouds into continuous surface meshes, which is a vital step in this study's methodology. Delaunay triangulation forms the core of this transformation (Luo et al., 2021). This technique was selected because it accurately represents the complex geometries of the chicken carcasses. The resulting mesh served as a bridge that facilitated the transition from the fragmented, discrete nature of a point cloud to a more cohesive, continuous representation. The Delaunay method connects adjacent data points within a cloud, sculpting a continuous mesh that preserves the nuanced contours and curvatures of the chicken carcass. This level of detail is crucial, because it establishes a baseline for generating a high-fidelity 3-D model that accurately reflects the physical characteristics of an object. The integrity of the resultant

mesh, crafted through Delaunay triangulation, significantly affects subsequent analyses, making it a foundational element for achieving accurate volume estimates and enhancing the robustness and credibility of the proposed methodology.

Surface Integration for Volume Estimation

The next step in estimating enclosed volume involves surface integration after constructing a 3-D surface mesh using advanced triangulation techniques. This method offers high accuracy and computational efficiency, making it a popular choice for real-time large-scale industrial applications (Labute, 2008).

Algorithmic Overview and Computation

1. Partitioning of the Mesh: In the case of a triangulated mesh, the main goal is to divide the surface mesh into smaller individual elemental regions, typically, triangles. This step is vital because the partitioning level of detail can affect both accuracy and computational speed.
2. Computational Steps for the Elemental Volume: For each elemental triangle, we calculated the volume of the tetrahedron formed using a reference point, which is often the origin. Let $\vec{A}$, $\vec{B}$, and $\vec{C}$ be the vertices of the triangle. The elemental volume V_{ele} is given by.

$$V_{\text{ele}} = \frac{1}{3!}\left|\left(\vec{A}-\vec{O}\right)\cdot\left(\left(\vec{B}-\vec{O}\right)\times\left(\vec{C}-\vec{O}\right)\right)\right| \quad (3)$$

(3) Total Volume Computation: The sum of all elemental volumes provides the total volume V_{total} .

$$V_{\text{total}} = \sum_{i=1}^{n} V_{\text{ele},i} \quad (4)$$

The underlying mathematical justification for this methodology is derived from Gauss's Divergence Theorem, which states that:

$$\iiint_V \nabla\cdot\vec{F}\ dV = \iint_S \vec{F}\ \cdot\ \hat{n}\ dS \quad (5)$$

Here, $\vec{F}$ is the vector field representing the mesh surface; $\nabla\cdot\vec{F}$ is its divergence; $dV$and dS are the differential volume and surface elements, respectively; and $\hat{n}$ is the outward unit normal to the surface S. To relate this to our computational process, we considered $\vec{F}$ as the vector field representing the divergence of the 3-D surface and $\hat{n}$ as the unit normal. This theorem provides the relationship between the volume integral over a region and the surface integral over the boundary of the region, thereby validating the proposed approach mathematically.

The algorithm operates with a time complexity of $O(n)$, where n denotes the number of elemental regions. By combining rigorous mathematical foundations with computational efficiency, surface integration has emerged as a reliable method to estimate the volume of chicken carcasses. This makes it an essential component for a broad range of poultry management applications, thus further confirming the validity of the proposed methodology.

Feature Extraction

Feature extraction is vital for the use of depth images in determining the volume of chicken carcasses. We carefully extracted 2-D and 3-D features and created a dataset that provided a comprehensive understanding of the geometry of chicken carcasses (Fig. 6). Research on meat quality has shown that geometric features, such as area, convex area, perimeter, eccentricity, surface area, orientation, and lengths of the major and minor axes are directly related to the assessment of meat quality and yield prediction (Penning et al., 2020). We selected 3-D features based on their effectiveness in volume estimation, shape description, and industrial applications, such as automated cutting. These features contribute unique, non-redundant information to the model, and enhance its predictive power and robustness.

2-D Geometric Features

1. Area: The "Area" measures the total number of pixel units occupied by the chicken carcass within a depth image, providing a quick and rough understanding of the carcass size. Precise area measurements are essential for accurately calibrating other geometric features, making subsequent analyses, or processing steps such as 3-D modeling or volume estimation.

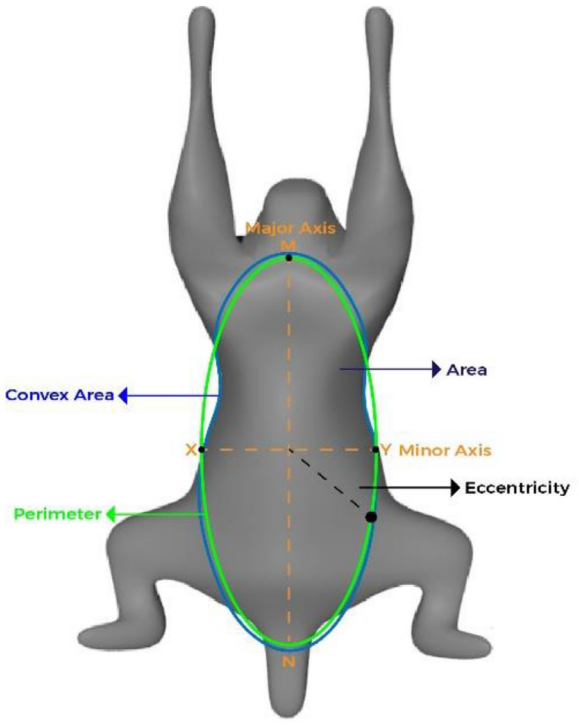

Figure 6. Illustration of extracted features of chicken carcasses.

Consistency in the area measurements across multiple samples can also help identify anomalies and outliers.

2. Perimeter: The "Perimeter" measures the distance around the outer boundary of the chicken carcass as captured in the depth image, providing a detailed view of the carcass's shape and irregularities. A large perimeter relative to the carcass area may indicate non-standard shapes, protrusions, or other anomalies crucial for quality control during processing. Perimeters are also critical in machine learning, serving as crucial features for categorizing carcasses based on their morphological complexities and informing decisions regarding automated sorting and grading systems. Edge detection techniques such as Canny are crucial for accurately determining perimeter (Canny, 1986).
3. Convex Area: The smallest convex polygon that can entirely enclose the chicken carcass in the image is determined, with the contrast between the convex area and the actual carcass area providing clues about the shape regularity of the carcass. If the values of the convex and carcass areas are similar, it suggests that the carcass has a standard or rounded shape. However, significant discrepancies indicated irregular shapes, which are critical for algorithm-based shape recognition.
4. The Major Axis Length: Which represents the longest possible line within the bounding ellipse of the chicken carcass on the image, is a crucial determinant in assessing the overall shape and primary orientation of carcasses. This understanding is essential for creating a foundational structure for the 3-D modeling of volume estimation.
5. Minor Axis Length: The smallest line length of the bounding ellipse of the carcass provides a comprehensive view of spatial orientation and elongation, which is critical for differentiating between elongated and rounded carcasses. This information can impact volume estimation when analyzed alongside the major axis length.
6. Eccentricity: Calculated from the major and minor axis lengths, eccentricity provides an insight into the roundness or elongation of the carcass, indicating chicken plumpness. A more circular carcass suggests greater meat volume, and an elongated shape may indicate different fat distributions that can affect the overall volume.

3-D Geometric Features

1. The Surface Area measures the external 3-D boundary, offering more than just a size representation. This served as an indicator of carcass morphology and texture. For example, 2 carcasses with similar volumes but different surface areas may suggest that one is smoother and that the other has more prominent features. Such differences can affect decisions related to skinning, deboning, or other processing-line operations. Additionally, the surface area can influence packaging, as the external spread of the carcass can affect the packaging material choice and design.
2. **Orientation:** Correct orientation of the carcass is essential for determining its position in a 3-D-captured environment. It involves placing the carcass in the correct position and standardizing the data for subsequent operations, such as cutting, grading, or imaging. Consistent orientation streamlines the process and reduces the risk of error. This feature was obtained through Principal Component Analysis (PCA), which is crucial for standardizing carcass positions and ensuring the generalizability of the model.

The selection of 2-D and 3-D features for chicken carcass volume estimation is a crucial aspect of our methodology, as it affects the accuracy and computational efficiency of our approach. Each feature serves a distinct yet interconnected role, resulting in a comprehensive representation that is suitable for industrial and analytical applications. The selection of the area, perimeter, and orientation as features is based on the fundamental geometric principles essential for size and shape estimation (Bhargava and Bansal, 2021; Nyalala, et al., 2021a). Previous studies on computational geometry and computer vision have highlighted the importance of these features in various object recognition and regression tasks (Chalidabhongse et al., 2006). Studies focusing specifically on volumetric estimations of agricultural and food technologies have supported the significance of these features (Concha-Meyer, et al., 2018; Nyalala et al., 2019,2021b). The selected features were not only comprehensive, but also computationally efficient, enabling real-time processing in high-speed industrial environments.

The three-dimensional morphological intricacies of the chicken carcasses were captured using binary-flagged voxel-based matrices, where each voxel was designated as "1" to indicate the presence of chicken carcass material or "0" to indicate its absence. This binary format simplifies the computational complexity and subsequent feature extraction processes. To identify surface voxels, a specialized variant of the Sobel operator, optimized for three-dimensional data, was employed (Woods and Gonzalez, 2008). This choice was driven by the proven effectiveness of the Sobel operator in edge detection, which offers greater accuracy in calculating surface areas than the other gradient-based methods.

To address the issue of spatial orientation as a source of variability in 3-D imaging, Principal Component Analysis (PCA) was used for standardization. PCA is an effective spatial normalization technique that mitigates orientation-induced variability by identifying and aligning the primary axes of variance within a 3-D dataset. This method was chosen because of its ability to reveal hidden structures within high-dimensional data and its applicability to reducing dimensions without significant information loss. The calculation of orientation

in a 3-D space generally involves determining the principal axes of the object. For depth images of chicken carcasses, one common approach is to use Principal Component Analysis (PCA) on the 3-D point cloud generated from the depth images. Orientation was calculated using the following steps:

1. Compute the mean point μ of X

$$\mu = \frac{1}{N}\sum_{i=1}^{N} x_i \tag{6}$$

2. The matrix X was centered by subtracting the mean values.

$$X_{\text{centered}} = X - \mu \tag{7}$$

3. The covariance matrix C of X_{centered} is calculated.

$$C = \frac{1}{N-1} X_{\text{centered}}^{T} \; X_{\text{centered}} \tag{8}$$

4. Compute the eigenvalues and eigenvectors of C.

$$C\vec{v} = \lambda\vec{v} \tag{9}$$

5. Eigenvectors were sorted in descending order according to their eigenvalues. The orientation of a chicken carcass can be described using the principal eigenvector corresponding to the largest eigenvalue. Here, C is the covariance matrix of the centered 3-D coordinates, and v are the eigenvectors. This principal eigenvector indicates the main orientation of the chicken carcass in 3-D space.

These methods were adopted to ensure accurate extraction of morphological features. This sets the stage for dependable large-scale analyses that satisfy the precision and computational efficiency requirements for industrial applications.

Table 3 provides a comprehensive and organized summary of the mathematical formulations used to extract specific features from the chicken carcass depth images. Each equation and its underlying methodology were based on established scientific principles to ensure validity and relevance in the context of chicken carcass analysis.

The second moments of the major and minor axes, represented by m_{major} and m_{minor}, respectively, effectively captured the pixel intensity distribution around the centroid of the image segment. These moments are essential for measuring the dispersion of the segments along their principal axes. Chicken carcasses are represented using 3-D voxels in the image space, leveraging the established principles of image processing (Petrou and Petrou, 2010) and linear algebra (Jacobson, 2013). This approach ensures analytical robustness for the evaluation of chicken carcasses.

Table 3. Mathematical formulations for deriving 2-D and 3-D features from carcass depth images.

No.	Feature	Equation
1	Area	$\sum$ (pixels_in_carcass) (10)
2	Perimeter	$\sum$ (edge_pixels_in_carcass) (11)
3	Convex area	$\sum$ (convex_hull_pixels) (12)
4	Major axis length	$\sqrt{8} \times m_{\text{major}}$ (13)
5	Minor axis length	$\sqrt{8} \times m_{\text{minor}}$ (14)
6	Eccentricity	$\sqrt{1 - \left(\frac{\text{Minor AxisLength}}{\text{MajorAxisLength}}\right)^2}$ (15)
7	Surface area (3-D)	$\sum$ (surface_voxels_in_carcass) (16)
8	Orientation	$\text{argmax}\vec{v}(\vec{v}^{T} \cdot C \cdot \vec{v})$ (17)

Modeling Approach for Carcass Volume Estimation

The primary objective of this study was to develop a grading system for the online volume estimation of chicken carcasses using computer vision and machine learning models. To achieve this, we carefully selected a multidimensional feature set from the depth images and 3-D reconstruction. Nine features were chosen, including six 2-D geometric attributes and three 3-D attributes, such as the volume derived from surface integration. These parameters served as inputs for the machine learning models. We followed a rigorous experimental design, adhering to the standard machine learning practices outlined by Bishop and Nasrabadi (2006). Our dataset of 40 randomly selected chicken carcass images was used for training and 20% of the samples were reserved for model validation during the training phase. The remaining 80% were used for post-validation testing. We explored various machine learning techniques for volume estimation, including but not limited to regression trees, Support Vector Regression (**SVR**), Gaussian Process Regression (**GPR**), ensemble methodologies, and various neural network architectures. Each model was subjected to rigorous training and evaluation.

Our study aimed to develop a robust and scientifically rigorous methodology for volume estimation in poultry that could serve as a foundation for future research in this interdisciplinary domain. Figure 7 presents the process of training and evaluating various machine learning regression models, which comprises three main steps. In Step 1, the dataset is randomly divided into training and testing sets. Hyperparameter tuning and optimization were performed on the training set using a k-fold cross-validation algorithm that protected against overfitting. Step 2 involved training the regression models using the optimized training set. Finally, Step 3 evaluates the performance of the trained models on the test set by employing specific statistical measures for the volume estimation.

Regression Trees. Three types of regression trees, fine, medium, and coarse, have distinct approaches for modeling chicken carcass volume estimation. Fine trees, with many branches and deep layers, excel at capturing intricate patterns but may lead to overfitting, where the model performs well on the training data but poorly on unseen data. Medium trees strike a balance, controlling complexity to generalize well without losing significant details. Coarse trees with shallow depths and fewer branches offer a high-level view, focusing on broad

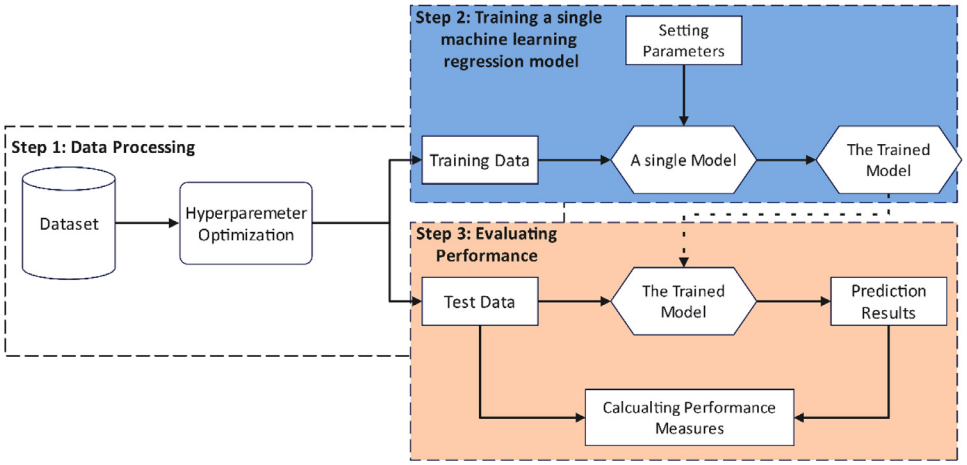

Figure 7. Training and evaluation process for single-regression models.

trends and key features, although potentially missing nuanced details (Loh, 2011). The choice between these models depends on the desired balance between interpretability and predictive accuracy, with fine trees favoring the latter, and coarse trees favoring the former.

The selection of trees requires a careful analysis of algorithms and hyperparameters. Fine trees were tuned using deeper levels and stricter splitting criteria, necessitating cross-validation to assess generalization to an independent dataset, and pruning to eliminate branches with limited predictive power. The medium trees were balanced in terms of flexibility and robustness, using moderate tuning. Coarse trees prioritize simplicity and set lower values for depth and branching to provide a broader overview. Algorithms were chosen based on the nature of the data and their implementation was rigorously assessed to align it with the intended level of detail.

Gaussian Process Regression. Gaussian Process Regression (**GPR**) is a probabilistic non-parametric Bayesian technique that has been widely applied to regression problems owing to its flexibility and simplicity (Quinonero-Candela, et al., 2007). The GPR approach facilitates Bayesian use of kernels during training by presupposing a GP before the functions (Okinda et al., 2020b). The covariance of the GP prior is dictated by a positive semi-definite kernel that optimizes its hyperparameters by maximizing the log-marginal-likelihood function (Williams and Rasmussen, 2006). This study utilizes various kernel functions, each with unique characteristics, such as Squared Exponential (eqn [18]), also known as the radial basis function, Matern 5/2 (eqn [19]), Rational Quadratic (eqn [20]), and exponential (eqn [21]), given their efficacy in handling multidimensional feature vectors and different kernels, and to enhance adaptability to tomato fruit volume estimation.

The Rational Quadratic Kernel, defined by scale length l and shape parameter α, adapts to multiple scaling behaviors in the data (Schulz, et al., 2018). The Squared Exponential Kernel, which is governed by the length scale l, yields smooth continuous curves. The Matérn 5/2 kernel, using a scale parameter l and fixed smoothness of 5/2, achieves a balance between smoothness and flexibility. The Exponential Kernel, controlled by a shorter length scale l, is suitable for modeling rapid transitions. The implementation of these kernels involves tuning specific hyperparameters. For a Rational Quadratic Kernel, the length scale l influences the range of correlations and the shape parameter α controls the weights of different scales. The Squared Exponential Kernel length scale l determines how closely the data points are correlated, whereas the Matérn 5/2 kernel's fixed smoothness and scale parameter l enable a balanced fit. The Exponential Kernel length scale l controls the decay of correlations and captures sharp changes in the data.

Support Vector Regression. Support Vector Regression (**SVR**) is a supervised ML technique used for regression analysis. This technique computes a hyperplane that effectively fits nonlinear data points (Okinda, et al., 2018). The hyperplane is responsible for maximizing the boundary around data points. The margin boundary is the distance between the nearest points and the hyperplane. A typical kernel functions as a hyperparameter by reading training data. We specifically explored the linear (eqn [22]), polynomial (eqn [23]), and Gaussian (eqn [24]) SVR variants given their flexibility and robustness for diverse data patterns, as detailed in Table 4. The choice of a kernel in SVR can significantly impact the adaptability and performance of the model (Nyalala et al., 2019), particularly for intricate datasets, such as ours. Linear kernels are effective for data exhibiting linear relationships and offer a high computational efficiency. Quadratic and cubic kernels allow the capture of polynomial relationships, adding flexibility to more complex patterns. Gaussian kernels, classified as fine, medium, or coarse, based on the bandwidth parameter, can be used to model nonlinear relationships with varying degrees of granularity. Fine Gaussian kernels capture subtle details, coarse kernels focus on broad trends, and medium kernels provide a balanced approach (Huang et al., 2012).

Implementing Support Vector Regression (**SVR**) models requires strategic selection of hyperparameters. A crucial hyperparameter is the regularization constant (C), which controls the balance between maximizing the

Table 4. Kernel equations for GPR and SVR models.

Model parameters	Kernel equations
Gaussian process regression	
Squared exponential	$k(x,x') = \exp\left(-\frac{x-x'^2}{2l^2}\right)$ (18)
Matern 5/2	$k(x,x') = \left(1+\frac{\sqrt{5}x-x'}{l}+\frac{5x-x'^2}{3l^2}\right) \exp\left(-\frac{\sqrt{5}x-x'}{l}\right)$ (19)
Rational quadratic	$k(x,x') = \left(1+\frac{x-x'^2}{2\alpha l^2}\right)^{-\alpha}$ (20)
Exponential	$k(x,x') = \exp\left(-\frac{x-x'}{l}\right)$ (21)
Support vector regression	
Linear	$k_l(x_i,x_j) = x_i^T x_j$ (22)
Polynomial	$k_Q(x_i,x_j) = (1+x_i^T,x_j)^d$ where, $d>0$ (23)
Gaussian	$k_G(x_i,x_j) = \exp\left(-\frac{x_i-x_j^2}{2\sigma^2}\right)$ *where* $\sigma>0$ (24)

margin and minimizing the regression error for linear kernels (Huang et al., 2021). Typical values of C range from 0.1 to 100. For quadratic and cubic kernels, tuning the degree of the polynomial and regularization is necessary. The degree (d) for quadratic kernels was set to 2, and for cubic kernels, it was set to 3. The coefficient values were tuned through cross-validation for both the quadratic and cubic kernels. Gaussian kernels are available in fine, medium, and coarse variations, as determined by the bandwidth parameter (σ). Smaller σ values indicate fine granularity, whereas larger σ values indicate coarse granularity (Huang et al., 2021). Cross-validation and grid search were utilized across all models to optimize these hyperparameters and select the best kernel that aligned with the data characteristics.

Kernel approximation regression. Two kernel approximation techniques were applied to capture the nonlinear relationships in the chicken carcass volume data. The least-squares kernel minimized the squared differences to facilitate flexible fitting of the volume data, even when nonlinear patterns were present. The SVM Kernel leveraging optimal hyperplanes identified subtle variations in carcass volume across various categories of chickens by employing optimal hyperplanes. Implementing these kernel methods requires precision in the hyperparameter tuning. For the least-squares kernel, selecting the kernel type and regularization parameters is vital for balancing fit and complexity. In the SVM Kernel, the choice of kernel function, cost parameter (C), and specific kernel parameters is critical, enabling the model to capture complex relationships without overfitting. These decisions were shaped by the unique characteristics of the chicken carcass volume data, ensuring a tailored approach to this estimation challenge.

Ensemble of Trees. Ensemble methods, specifically, bagging and boosting trees, have been developed and utilized. Bagged trees employ bootstrap aggregation to create an ensemble of samples, reduce model variance, and enhance stability (Sutton, 2005). This is particularly useful when the data exhibits strong fluctuations or noise. However, boosted trees aim to minimize bias and variance through sequential learning (Sutton, 2005). Each tree focuses on the errors made by the preceding trees. The adaptability of this method allows it to capture intricate patterns and subtleties within the data, making it well-suited for complex nonlinear relationships inherent in chicken carcass volume estimation.

Implementing bagged and boosted trees for chicken carcass volume estimation requires careful consideration of algorithms and hyperparameters. Cross-validation techniques were employed to optimize the number of trees, tree depth, and node-splitting criteria for bagged trees, while avoiding overfitting. For boosted trees, selecting appropriate algorithms, such as AdaBoost or Gradient Boosting, and tuning the learning rates, tree depth, boosting iterations, and regularization parameters are crucial. These implementations were customized to address the specific characteristics and challenges of the data, demonstrating a thoughtful and insightful approach.

Regression Neural Networks. Several regression neural network architectures have been investigated for chicken carcass volume estimation, each tailored to unique complexities within the data. Narrow neural networks with fewer neurons are appropriate for modeling linear relationships and basic patterns, thereby minimizing the risk of overfitting. Wide- neural-network models intricate nonlinear relationships within a dataset, thereby providing a more comprehensive representation. Medium neural networks provide flexibility and serve as a bridge between simplicity and complexity. Bilayered and Trilayered neural networks extract high-level features by using hierarchical learning.

The selection and tuning of the hyperparameters were performed accurately, considering the specific task. For example, the number of neurons in Narrow, Wide, and Medium neural networks have been optimized to match the level of complexity of the relationships within the data. The activation functions were chosen based on the data distribution characteristics, and the learning rate adjustments ensured a steady convergence during training. To prevent overfitting, regularization techniques, such as dropout, have been applied to Bilayered and Trilayered neural networks. Cross-validation guided this fine-tuning process, resulting in a robust estimation model that accounted for variations in chicken carcass shape and size.

Artificial Neural Networks (ANNs). ANNs, which are composed of interconnected neurons and are inspired by the architecture of the human brain, have been used to solve complex problems (Huang, et al., 2007). ANNs effectively model the complex nonlinear relationships between the inputs and outputs. The learning process in ANNs involves a loss function that is minimized using various optimization algorithms (Okinda, et al., 2020a). Training continues until specific termination criteria or stop conditions are satisfied (Samarasinghe, 2016). We implemented multilayer perceptron (**MLP**) networks comprising input, hidden, and output layers, and trained them using Levenberg−Marquardt, Bayesian regularization, and scaled conjugate gradient algorithms (Fig. 8). Each algorithm exhibits unique strengths in addressing complex data structures, making them ideal for our objective. The network was tested with three powerful optimizers: adaptive moment estimation

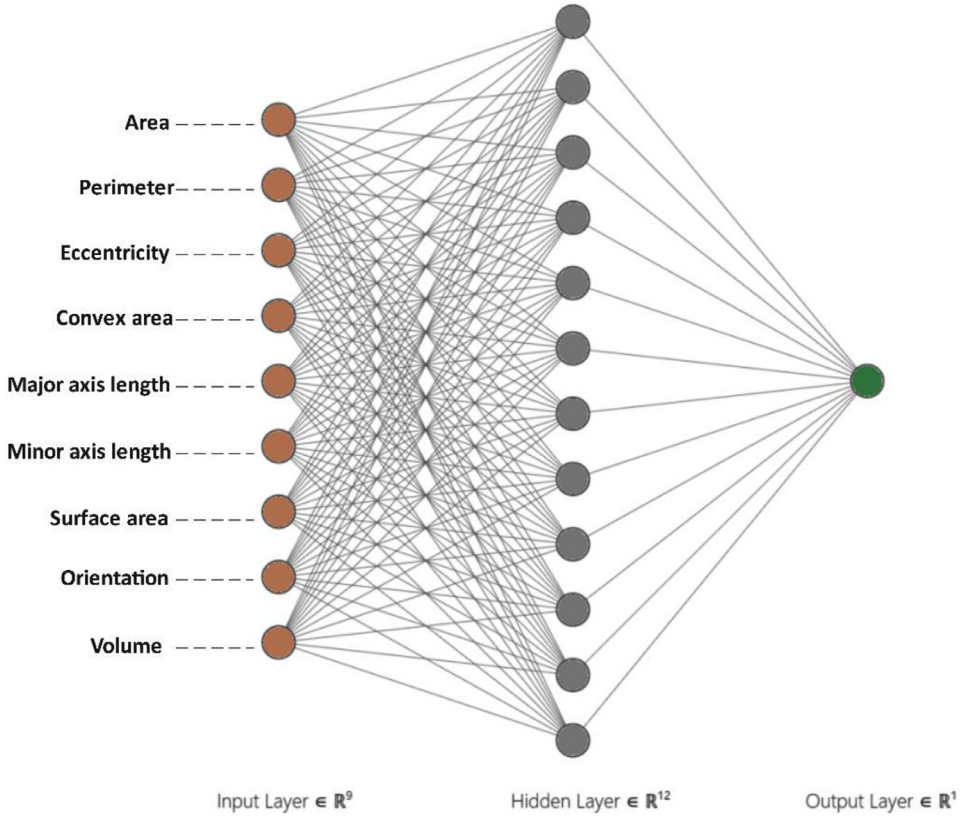

Figure 8. ANN model training.

(**Adam**), stochastic gradient descent (**SGD**), and limited memory Broyden−Fletcher−Goldfarb−Shanmo (**L-BFGS**). The tests showed that the Adam optimizer enriches the results owing to its adaptive nature, allowing Adam to converge faster and more efficiently to obtain optimal solutions for regression problems. Within the ANN framework, the Levenberg-Marquardt algorithm converges quickly to a solution by combining the steepest descent and Gauss-Newton methods (Gavin, 2019). In addition, Bayesian Regularization has been applied to control overfitting by introducing statistical constraints on the weight parameters of the network (Burden and Winkler, 2009). A Scaled Conjugate Gradient algorithm was also implemented, which was particularly effective in tackling problems by adapting the step size to improve the convergence.

These algorithms were carefully implemented and tuned using an ANN to ensure their precision. The Levenberg-Marquardt method was optimized using fine-tuned damping factors to adjust the sensitivity of the method to the problem shape. Bayesian Regularization requires specific priors, noise-level tuning, balancing fit, and complexity. The Scaled Conjugate Gradient was carefully parameterized using convergence criteria based on the gradient norms and function values. A 10-fold cross-validation was consistently applied during training, and the dataset was partitioned into ten subsets to obtain a robust estimate of model performance. This precise attention to implementation and tuning ensured that the models were efficient and well suited to the demands of the problem.

Performance Metrics for Carcass Volume Estimation Models

To address the challenge of accurate volume estimation, we evaluated various machine learning models based on specific criteria, including accuracy, computational efficiency, and adaptability to diverse datasets. The models were trained and tested multiple times to eliminate outliers, and the results were averaged to reduce bias. The performance metrics used to evaluate the performance of the models included the R-squared, adjusted R-squared, RMSE, MAE, MSE, and ARE, which are explained in the subsequent section.

Root Mean Square Error **(RMSE)**: The RMSE is a commonly renowned evaluation technique for regression analysis because of its sensitivity to significant deviations, which makes it a reliable tool for applications such as carcass volume estimation. Its widespread acceptance in predictive studies adds credibility as attested by Chai and Draxler (2014). The RMSE formula calculates the average deviation between the predicted and actual values by taking the square root of the mean squared error. RMSE outputs a single value that represents the total error of the model. Owing to its scale-dependent features, it is primarily used to assess the quality of different ML algorithms or check the quality of a single algorithm over different datasets, thereby ensuring the reliability of the model. Its formula is:

$$\mathrm{RMSE} = \sqrt{\frac{1}{n}\sum_{i=1}^{n}(y_i - \hat{y}_i)^2} \tag{25}$$

The Mean Squared Error **(MSE)** and Mean Absolute Error **(MAE)** are popular metrics for evaluating the predictions of regression models. MSE computes the average squared difference between the estimated chicken carcass volume values and actual values. MAE is the most popular criterion for evaluating the performance of the ML model, particularly in regression cases (Korohou, et al., 2020). It is less sensitive to outliers, making it a better metric for evaluating the best model for a given problem. MAE computes the average absolute value difference between the model-predicted and actual values, where each set of differences has an equal weight. MAE evaluates the model performance with a single value ranging from zero to infinity. A single MAE value represents the overall performance of an algorithm. When the output shows fewer values, the model has better performance or goodness of learning, indicating that the model's estimated values are closer to the actual values (Kuhn and Johnson, 2013). Combining MSE and MAE in the evaluation provides a more detailed understanding of the accuracy of a model, considering both the squared and absolute discrepancies (Chicco, et al., 2021). The formula for MSE is as follows:

$$\mathrm{MSE} = \frac{1}{n}\sum_{i=1}^{n}(y_i - \hat{y}_i)^2 \tag{26}$$

The mathematical representation of MAE is given as

$$\mathrm{MAE} = \frac{1}{n}\sum_{i=1}^{n}|y_i - \hat{y}_i| \tag{27}$$

Coefficient of Determination **($\mathbf{R}^2$)**: R-squared, or the coefficient of determination, is a statistical technique used to evaluate the quality of a regression algorithm. R^2 measures the goodness of fit, which determines how the data fits the regression model. It has a scale between 0 and 1, representing none or all the variances in the target variable, and is explained by the input variable(s) (James, et al., 2013). Understanding the variability in chicken carcass size and shape aids in comprehending the proportion of observed variance explained by the model (Di Bucchianico, 2008). The mathematical representation of this metric is as follows.

$$\mathrm{R}^2 = 1 - \frac{\sum_{i=1}^{n}(\widehat{y}_i - y_i)^2}{\sum_{i=1}^{n}(y_i - \overline{y}_i)^2} \tag{28}$$

The Adjusted Coefficient of Determination **($\mathbf{R}^2_{\mathbf{adj}}$)** is a critical performance metric in chicken carcass volume estimation, as it measures the proportion of variation in carcass volume predictions explained by the model after accounting for the number of independent variables. This can be mathematically represented as

$$\mathrm{R}^2_{\mathrm{adj}} = 1 - \frac{(1 - R^2)(n-1)}{n-k-1} \tag{29}$$

where n represents the observed carcasses and k denotes the independent variables in the model. The adjusted R-squared value can help select a model that balances accurate predictions with the complexity introduced by the variables, thus selecting a model that effectively capturing the factors affecting chicken carcass volume estimation.

The Average Relative Error **(ARE)** calculates the average error between the estimated and actual chicken carcass volumes relative to the actual volumes. A lower ARE indicates a better model accuracy, which is important for pricing and quality control. ARE is mathematically calculated as follows:

$$\mathrm{ARE} = \left(\frac{\frac{1}{n}\sum_{i=1}^{n}|y_i - \hat{y}_i|}{|y_i|}\right) \times 100\% \tag{30}$$

where ARE is the average relative error of the i^{th} chicken carcass. where, n is the total number of carcasses. y_i represents the actual volume of the i^{th} chicken carcass and $\widehat{y}_i$ is the estimated volume for the same carcass, as predicted by the model. This formula computes the average relative error across all n carcasses and provides a single value (**ARE**), that indicates the overall accuracy of the model.

We compared our model's performance with an established benchmark by conducting paired t-tests using the strict significance threshold of $P < 0.05$ (Hsu and Lachenbruch, 2014). This study contributes significantly to chicken carcass volume estimation by combining rigorous techniques with innovative approaches. The impact of this research extends beyond simple carcass grading, as it has the potential to improve poultry industry standards and advance the development of food quality and security measures.

Methodological Flowchart for Chicken Carcass Volume Estimation

To provide a clear understanding of the procedures employed in this study, Figure 9 presents a comprehensive flowchart that outlines the essential steps, starting with depth image acquisition, progressing to image processing and 3-D reconstruction, and resulting in the feature extraction. This study rigorously evaluated twenty-five regression models for volume estimation, each based on a predefined performance metric. In addition, the most efficient model was evaluated for its real-time processing capabilities for volume estimation. This flowchart functions as a map, directing the reader through the methodology described in the results section.

In the proposed method, the 3D reconstruction process begins with the acquisition of depth images using a Kinect v2 sensor. These depth images were then converted into point clouds representing the spatial geometry of chicken carcasses. Point clouds were filtered to remove noise and outliers, followed by a surface reconstruction step using the Poisson surface reconstruction algorithm. This algorithm was chosen for its robustness in handling incomplete data and noise, thus providing a smooth and accurate 3D model of carcasses.

Once the 3D models were reconstructed, we extracted a set of 3D features, such as the volume and surface

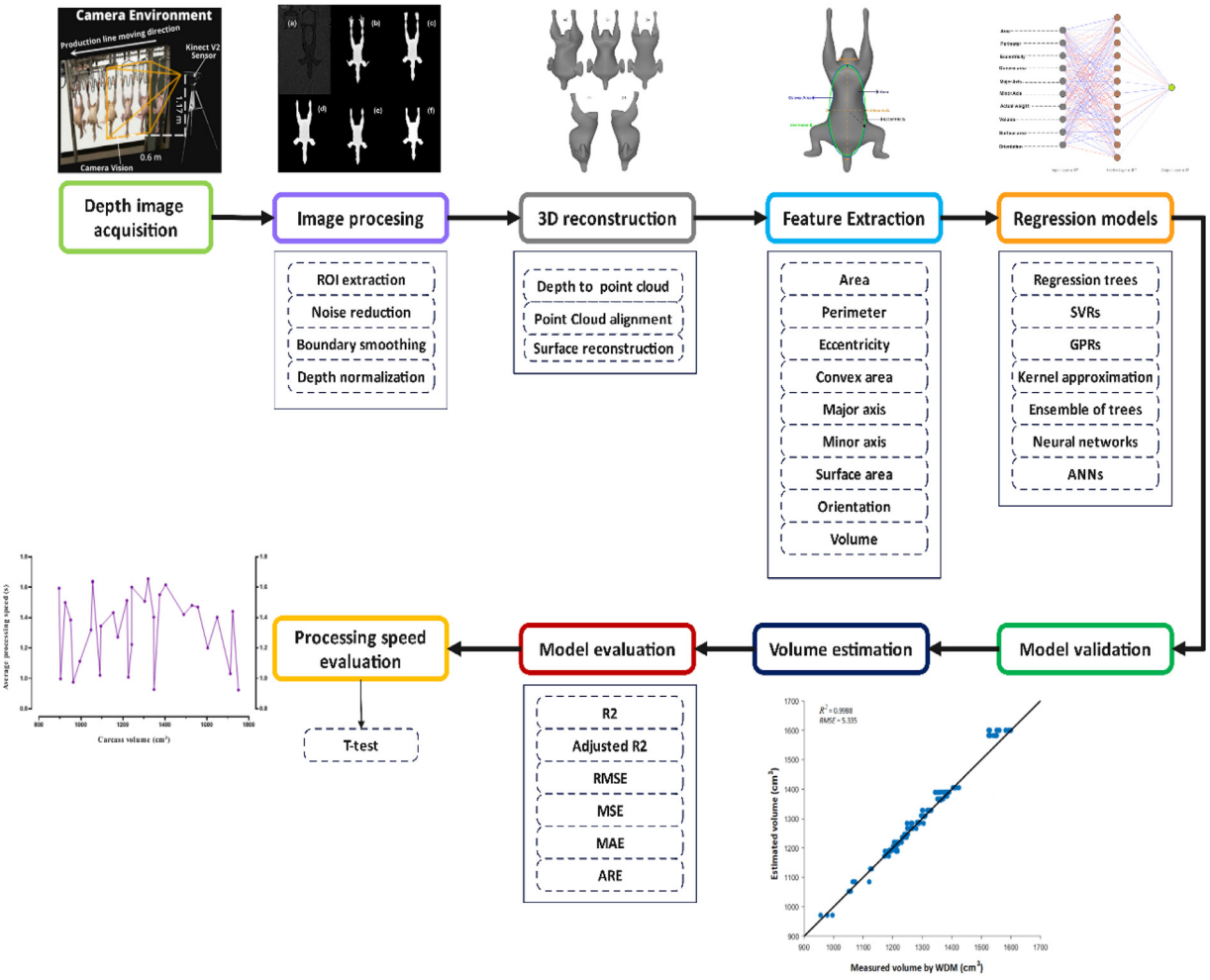

Figure 9. Comprehensive methodology flowchart for chicken carcass volume estimation.

area, along with 2D features derived from the depth images. These features were then used as inputs for the machine learning models. The models were trained on a dataset that included these features along with ground-truth measurements of the carcass volume. The integration of both 2D and 3D features allows the models to leverage depth data effectively, thereby capturing the intricate geometries of carcasses that are crucial for accurate volume estimation.

Building on detailed comprehensive methodologies, we present the outcomes of our model evaluations, illustrating the practical applicability and precision of the proposed solution.

RESULTS

Results of Depth-to-Point Cloud Conversion Calibration

After carefully evaluating the intrinsic camera parameters through rigorous calibration, we measured the effectiveness of adjusting these parameters using the RMSE. As shown in Table 5, the RMSE improved significantly from 3.9 mm in the initial phase to 2.8 mm post-optimization. To further reinforce this improvement, we performed a paired t-test and obtained a p-value of less than 0.05. This confirms that the reduction in RMSE is statistically significant. The RMSE was calculated based on a sample of 1000 data points carefully selected to represent various scenarios, including different orientations and distances of chicken carcasses from the Kinect v2 sensor.

The graph depicted in Figure 10 displays a line chart that highlights the trend of the root-mean-square error (RMSE) values across calibration iterations, thereby offering additional confirmation of the efficacy of our calibration optimization process. Our methodology was both sturdy and reliable, as evidenced by an RMSE of 2.8 millimeters, which falls well within the permissible range for three-dimensional reconstruction and estimation of volume for chicken carcasses.

Table 5. RMSE results for depth-to-point cloud conversion calibration.

Calibration method	RMSE (mm)	Confidence interval (95%)	Data points
Initial calibration	3.9	± 0.3	1000
Optimized calibration	2.8	± 0.1	1000

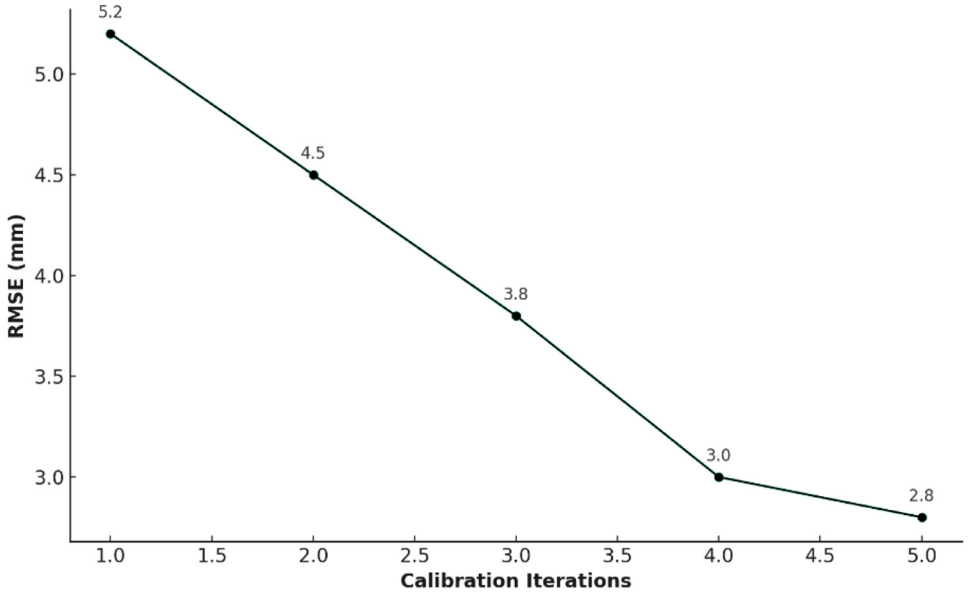

Figure 10. Trends in RMSE values across calibration iterations.

Results of 3-D Surface Reconstruction

The 3-D model reconstructed from the point clouds of the chicken carcasses is shown in Figure 11. The model appears thorough, indicating its ability to handle challenges, such as occlusions in depth images. The anterior (A and B), posterior (C), and lateral (D and E) views shown in Figure 11 provide a comprehensive understanding of model geometry and structure. This reconstructed model illustrates the potential of depth images to create accurate and detailed 3-D models, which is particularly important in applications such as volume estimation.

Results of Tree-Based Models for Carcass Volume Estimation

The accuracy of estimating the volume of chicken carcasses has significant implications for the meat industry, affecting metrics and processing techniques. Given their straightforward nature, regression tree models have been explored for suitability. This section evaluates three regression tree models with varying levels of detail, namely fine trees (detailed splits), medium trees (moderate granularity), and coarse trees (broad data splits) summarized in Table 6. The Fine Tree led in precision with an R^2 value of 0.9591 and an RMSE value of 21.532 cm^3, demonstrating a robust correlation between the predicted and actual volume values. The R^2_{adj} value of the model was 0.9488, indicating a minor deviation from the actual values. The Medium Tree had commendable R^2 and RMSE values of 0.9289 and 24.056 cm^3, respectively, confirming the reliability of the predictions. Although not as precise as the other models, the Coarse Tree model exhibited significant predictive capabilities, with R^2 and RMSE values of 0.9059 and 29.189 cm^3, respectively. The R^2_{adj} value of 0.9252 reinforces its practical relevance for volume estimation.

The results demonstrate the superiority of fine trees in terms of precision and reliability. Nevertheless, the consistency across all models underscores the versatility of regression trees for volume estimation tasks. Such findings may lead to further optimization, potentially combining features from all models to enhance accuracy. The scatter plots provide a direct visual assessment of the predictive accuracy of the model. In Figure 12, we compare the estimated volumes from the regression tree models with those derived from the Water Displacement Method (WDM) using the fine tree regression model. This comparison served as a crucial validation tool.

Results of Support Vector Regression for Carcass Volume Estimation

The assessment of the Support Vector Regression (**SVR**) model for estimating chicken carcass volumes provides insightful observations, as shown in Table 7. For our linear framework, Linear SVR yielded an R^2 value of 0.9088, an R^2_{adj} of 0.7382, and an RMSE value of 28.773 cm^3. For polynomial configurations, Quadratic SVR demonstrated an improved R^2 value of 0.9119, with R^2_{adj} and RMSE values of 0.9117 and 23.426 cm^3, respectively. The Cubic SVR further refined the model, recording R^2, R^2_{adj}, and RMSE values of 0.9505, 0.9117, and 20.901 cm^3, respectively. Next, we explored Gaussian kernel types, and Fine Gaussian SVR emerged as the top performer with R^2, R^2_{adj}, and RMSE values of 0.9928, 0.9927, and 12.978 cm^3, respectively. The Medium Gaussian SVR had acceptable R^2 and RMSE values of 0.9765 and 19.987 cm^3, respectively, whereas the Coarse Gaussian SVR had a lower R^2 and higher RMSE values of 0.8921 and 32.807 cm^3, respectively. Overall, the superior performance of the Fine Gaussian SVR highlights its potential as a crucial tool for poultry processing volume estimations. Given its precision,

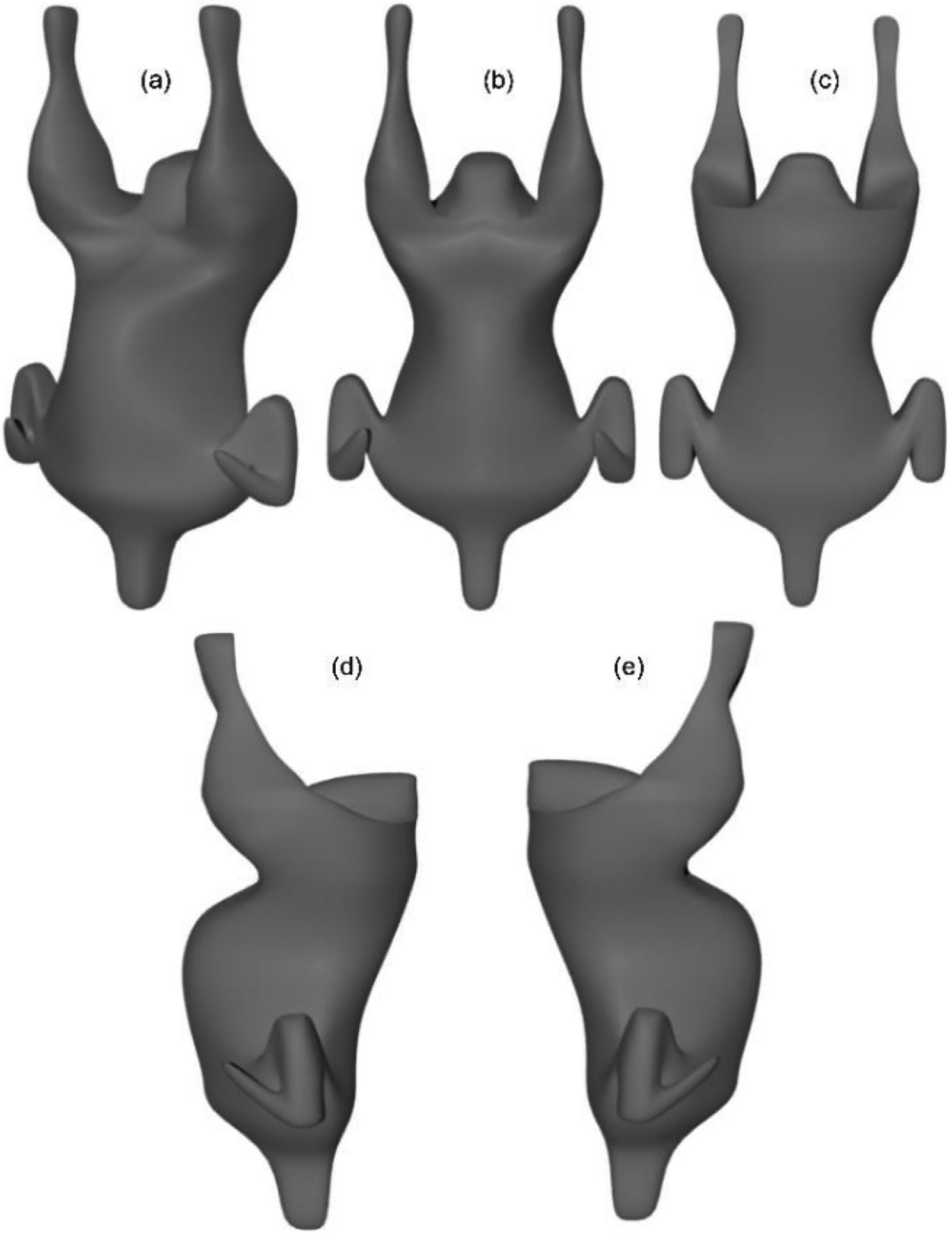

Figure 11. 3-D surface reconstruction results.

exploring its application in related domains can yield groundbreaking results.

Figure 13 presents a scatter plot illustrating the correlation between the estimated volumes, as the Fine Gaussian SVR kernel estimates, and the measurements derived from the water displacement method (**WDM**). In an ideal scenario, data points should adhere closely to a diagonal line, indicating precise volume estimation. Any deviation from this line suggests potential inaccuracies in predictions. This visual representation highlights the performance metrics of the Fine Gaussian SVR kernel and underscores its applicability in generating tangible, real-world insights, particularly in poultry processing volume assessments.

Table 6. Performance results of tree-based regression models in volume estimation.

No.	Regression models	R^2	RMSE (cm^3)	R^2_{adj}
1	**Fine tree**	**0.9591**	**21.532**	**0.9488**
2	Medium tree	0.9289	24.056	0.9286
3	Coarse tree	0.9059	29.189	0.9252

The boldface shows the model with the highest accuracy.

Results of Gaussian Process Regression Models for Carcass Volume Estimation

Gaussian Process Regression (**GPR**), known for its adaptability, provides valuable insights into chicken carcass volumes (Table 8). The evaluation of various GPR kernel models reveals distinct performance characteristics. The Rational Quadratic GPR displayed a strong predictive capability, with R^2, RMSE, and R^2_{adj} values of 0.9983, 7.016 cm^3, and

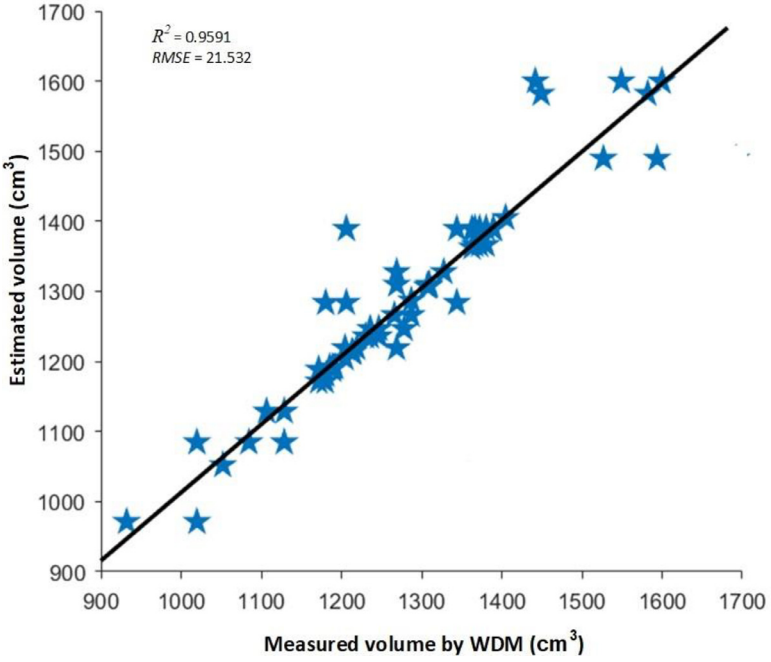

Figure 12. Scatter plot of fine-tree regression model.

Table 7. Performance results of support vector regression models in volume estimation.

No.	Regression models	R^2	RMSE (cm^3)	R^2_{adj}
1	Linear SVR	0.9088	28.773	0.7382
2	Quadratic SVR	0.9119	23.426	0.9117
3	Cubic SVR	0.9505	20.901	0.9504
4	**Fine Gaussian SVR**	**0.9928**	**12.978**	**0.9927**
5	Medium Gaussian	0.9765	19.987	0.9764
6	Coarse Gaussian	0.8921	32.807	0.6313

The boldface shows the model with the highest accuracy.

0.9980, respectively. The Squared Exponential GPR achieved an R^2 value of 0.9980, despite having a slightly higher RMSE value of 9.821 cm^3 than that of the Rational Quadratic GPR. However, an R^2_{adj} value of 0.9976 confirmed its generalization capabilities. The performance of the Matern 5/2 GPR was comparable, with R^2, RMSE, and R^2_{adj} values of 0.9982, 8.475 cm^3, and 0.9979, respectively. Exponential GPR was the most precise, with R^2 and RMSE values of 0.9984 and 6.113 cm^3, respectively, which were the lowest among the evaluated models, indicating its potential for use

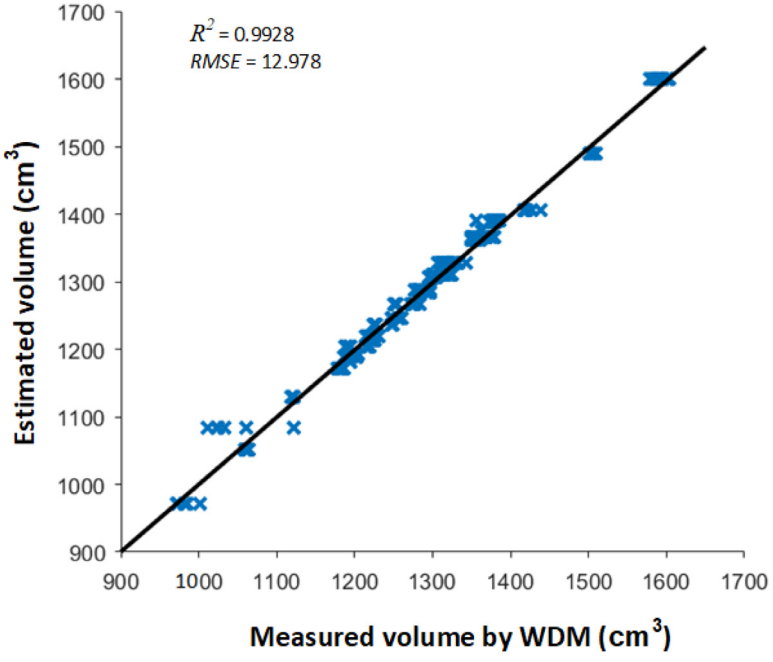

Figure 13. Scatter plot of the Fine Gaussian SVR model.

Table 8. Performance results of Gaussian process regression models in volume estimation.

No.	Regression models	R^2	RMSE (cm^3)	R^2_{adj}
1	Rational Quadratic GPR	0.9983	7.016	0.9980
2	Squared Exponential	0.9980	9.821	0.9976
3	Matern 5/2 GPR	0.9982	8.475	0.9979
4	**Exponential GPR**	**0.9984**	**6.113**	**0.9982**

The boldface shows the model with the highest accuracy.

in poultry processing volume predictions. An R^2_{adj} value of 0.9982 further confirmed its effectiveness. In conclusion, although each GPR kernel model has its strengths, Exponential GPR stands out in terms of precision, making it a promising choice for poultry processing volume predictions.

Figure 14 illustrates the performance of the Exponential Gaussian Process Regression (**E-GPR**) model in estimating chicken carcass volumes using a scatter plot. The x-axis represents the volumes predicted by the E-GPR model, and the y-axis represents the volumes measured using the Water Displacement Method (**WDM**). Each data point in the plot corresponds to a distinct carcass sample. Most of these points clustered around the diagonal, indicating the accuracy of the E-GPR model. Although there are inevitable deviations from this line owing to inherent variability and potential measurement errors, the overall trend confirms the reliability of the E-GPR model for predicting carcass volumes. This close alignment between the predicted and actual volumes underscores the robustness of the E-GPR model for practical applications.

Results of Kernel Approximation Models for Carcass Volume Estimation

In high-dimensional datasets, kernel approximation methods tailored for regression analyses have proven to be effective when the traditional kernel approach becomes unfeasible. In this study, a focused examination was conducted on two prominent kernel approximation models: the least-squares kernel and SVR kernel presnted in Table 9. The least-squares kernel had an R^2 value of 0.9639, indicating that it was proficient in accounting for approximately 96.39% of the variance in the dataset. The RMSE and R^2_{adj} values of 24.044 $cm^3$and 0.9638, respectively, further supported this conclusion. Conversely, the SVR Kernel registered R^2, and R^2_{adj} values of 0.8925 and 0.8917, respectively, which were paired with a higher RMSE value of 47.457 cm^3, suggesting that its predictions contained a larger error magnitude than the true values. The differences in the performance metrics between these models can be attributed to their underlying mathematical frameworks, potentially indicating that the dataset aligns more favorably with the constructs of the least squares kernel.

The scatter plot in Figure 15 compares the measured volume (as per the WDM method) on the x axis with the estimated volumes on the y axis. The ideal scenario would display data points aligned along a 45-degree diagonal, indicating perfect correlation between the estimates and measurements. The proximity of data points to this line reflects the predictive accuracy of the model. A tight cluster around this diagonal signifies accurate predictions, whereas deviations or broader scattering indicates discrepancies. The pattern and spread of these deviations can provide insights into the prediction challenges of the model.

Results of the Ensemble of Trees Models for Carcass Volume Estimation

An ensemble of tree models, including bagged and boosted trees, were evaluated for their regression performance as shown in Table 10. The bagged tree model

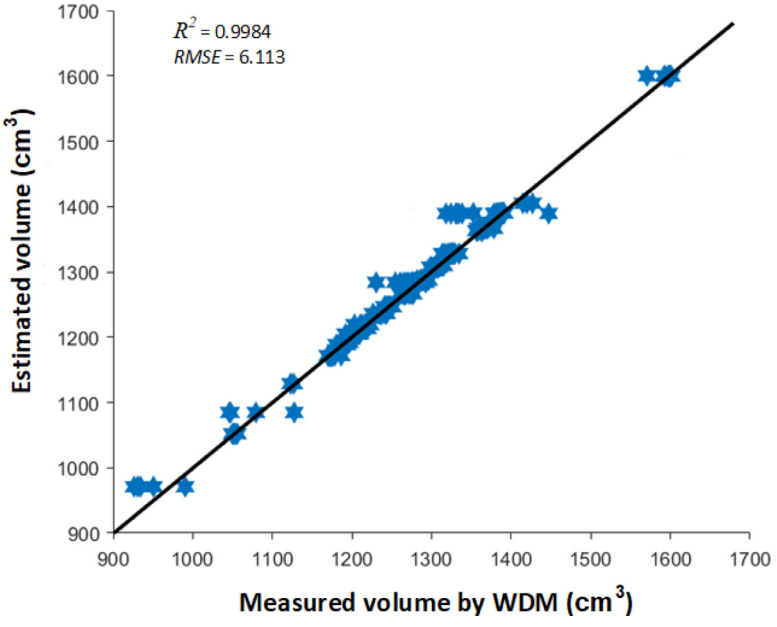

Figure 14. Scatter plot of the exponential GPR model.

Table 9. Performance results of kernel approximation models in volume estimation.

No.	Regression models	R^2	RMSE (cm^3)	R^2_{adj}
1	**Least Squares Kernel**	**0.9639**	**24.044**	**0.9638**
2	SVR kernel	0.8925	47.457	0.8917

The boldface shows the model with the highest accuracy.

Table 10. Performance results of the ensemble of trees models in volume estimation.

No.	Regression models	R^2	RMSE (cm^3)	R^2_{adj}
1	**Bagged trees**	**0.9988**	**5.335**	**0.9987**
2	Boosted trees	0.9733	10.001	0.9732

The boldface shows the model with the highest accuracy.

achieved an R^2 value of 0.9988, indicating its ability to explain a sizable proportion of the variance in the dataset. The low RMSE value of 5.335 cm^3 further confirms the accuracy of the predictions. In addition, the R^2_{adj} value of 0.9987 highlights the efficacy of the model in generalizing training data. By contrast, the boosted tree model achieved an R^2value of 0.9733. Although its performance was commendable, a higher RMSE value of 10.001 cm^3 suggests potential prediction inaccuracies. The model's R^2_{adj} value of 0.9732 confirms its ability to generalize the training data. However, the complexity of the boosting techniques can compromise their predictability. Overall, the bagged tree model demonstrated greater consistency and precision in volume estimation than its boosted counterpart did.

Figure 16 shows the predictions of the bagged tree model through a scatter plot, with the x-axis listing the model's volume estimates and the y-axis showing the volume measured using the WDM method. The data points in the plot indicate the reliability and accuracy of the proposed model, respectively.

Results of Regression Neural Networks Models for Carcass Volume Estimation

Assessing the architecture of regression neural network models sheds light on its impact on prediction accuracy. The configuration of each model differed, leading to variations in predictive capability, as demonstrated by the metrics listed in Table 11. The narrow neural network exhibited significant data variability with an R^2 value of 0.9760. However, its precision could be refined, given its RMSE and R^2_{adj}values of 23.6745 c m^3 and 0.9759, respectively. The wide and medium neural networks were the top performers, with the wide model boasting a superb R^2 value of 0.9914, lower RMSE value of 14.171 cm^3, and consistent R^2_{adj} value of 0.9912. The medium neural network yielded an R^2 value of 0.9922, which decreased the RMSE to 13.443 cm^3, accompanied by an R^2_{adj} value of 0.9920. These models demonstrate the benefits of expanding the networks in specific scenarios. Although Bilayered and Trilayered neural networks introduce additional depth to the architecture, their performance metrics suggest a trade-off between complexity and accuracy.

The Bilayered neural network achieved R^2, RMSE and R^2_{adj} values of 0.9869, 17.533 cm^3, and 0.9868, respectively. Although deeper, the trilayered neural network did not significantly outperform its bilayered counterpart, with R^2, RMSE and R^2_{adj} values of 0.9887, 16.2842 cm^3, and 0.9882, respectively. In summary, increasing the depth of neural networks can expand the model capacity, but does not guarantee improved performance. Wide and Medium neural networks have emerged as balanced solutions for managing the trade-off between performance and complexity. Further refinement of the configurations and hyperparameters may yield improved results for these architectures.

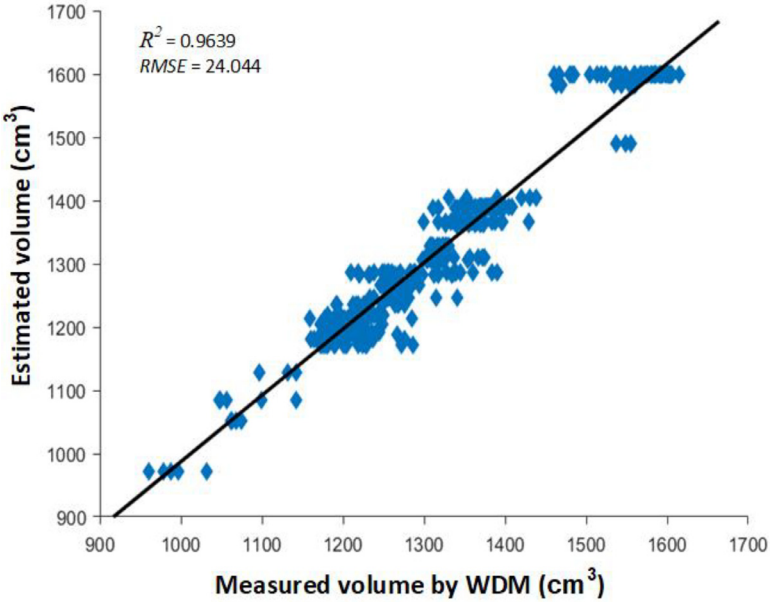

Figure 15. Scatter plot of least-squares kernel model.

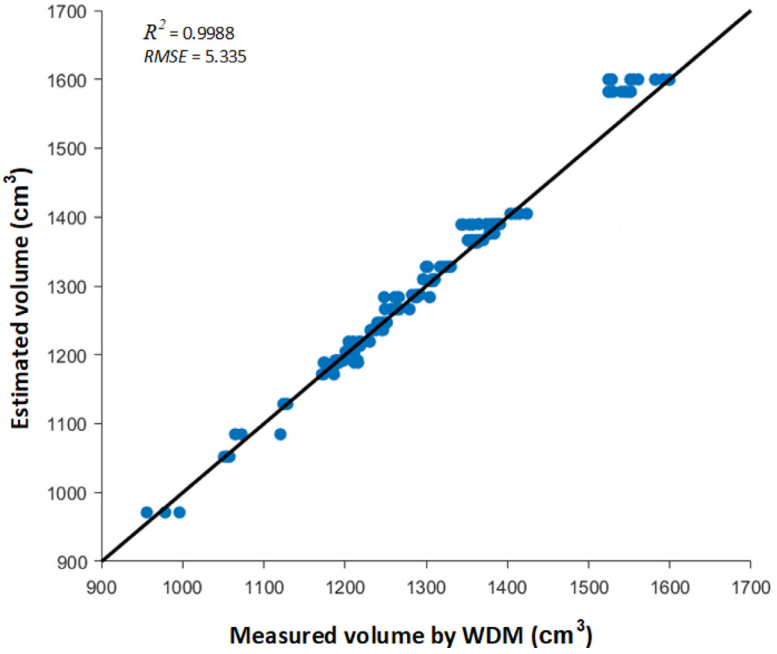

Figure 16. Scatter plot of the bagged tree model.

Table 11. Performance results of regression neural network models in volume estimation.

No.	Regression models	R^2	RMSE (cm^3)	R^2_{adj}
1	Narrow neural network	0.9760	19.674	0.9759
2	Wide neural network	0.9914	14.171	0.9912
3	**Medium neural network**	**0.9922**	**13.443**	**0.9920**
4	Bilayered neural network	0.9869	17.533	0.9868
5	Trilayered neural network	0.9887	16.284	0.9882

The boldface shows the model with the highest accuracy.

Figure 17 presents a scatter plot comparing the estimated volume values of the best-performing medium neural network predicted against the actual volume measurements obtained using the water displacement method (**WDM**). The x-axis displays the estimated volumes and the y-axis anchors these predictions to reality by showing the WDM-derived measurements. Given the status of the medium neural network as a top performer, this plot is crucial. This underscores the predictive power of the proposed model, and highlights its real-world relevance. The closeness of the points to the diagonal could be a testament to the potential of the model for practical poultry volume estimation, offering insights into its theoretical efficiency and practical utility.

Results of Artificial Neural Networks Models for Carcass Volume Estimation

The evaluation of different Artificial Neural Network (**ANN**) models, including Levenberg-Marquardt,

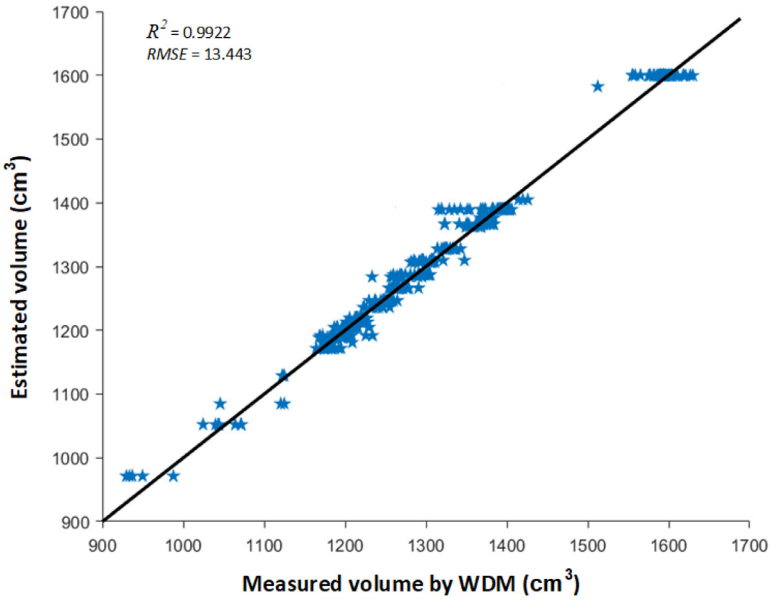

Figure 17. Scatter plot of medium neural network model.

Table 12. Performance results of artificial neural network models in volume estimation.

No.	Regression models	No. of Neurons	R^2	RMSE (cm^3)	R^2_{adj}
1	Levenberg-Marquardt	12	0.9892	15.890	0.9890
2	**Bayesian regularization**	**12**	**0.9910**	**14.539**	**0.9908**
3	Scaled conjugate gradient	12	0.9199	43.296	0.9193

The boldface shows the model with the highest accuracy.

Bayesian regularization, and scaled conjugate gradient in regression tasks, revealed varied performance levels as detailed in Table 12. The Levenberg-Marquardt model with an R^2 value of 0.9892 successfully captured 98.92% of the data variability. The precision of the model was further evident with a low RMSE value of 15.890 cm^3. The Bayesian Regularization model, with an R^2 value of 0.9890 indicated consistent performance, even when considering the number of predictors. A high R^2 value of 0.9910 and a low RMSE value of 14.539 cm^3 signify a high accuracy in volume estimation. The ability of the model to generalize effectively across datasets was supported by its high R^2_{adj} value of 0.9908. In contrast, the Scaled Conjugate Gradient model underperforms, with an R^2 value of 0.9199, suggesting that it might fail to capture some complexities in the dataset. A high RMSE value of 43.296 cm^3 indicated a potential predictive accuracy gap. The R^2_{adj} value of 0.9193 further underscores these challenges.

Based on the presented metrics, the Levenberg-Marquardt and Bayesian regularization models demonstrated improved predictive capabilities and stability compared to the Scaled Conjugate Gradient model. The architecture or training parameters can be modified to enhance the performance of the latter method. Further investigations using real-world validation sets or advanced ANN architectures may yield more refined models.

Figure 18 displays a scatter plot that compares the estimated volumes from the Bayesian Regularization model (x-axis) with the actual volumes measured using the Water Displacement Method (**WDM**) (y-axis). Each point in the plot represented a single carcass. This scatter plot evaluates the accuracy of the Bayesian Regularization model and helps to identify potential areas for improvement and the nature of the errors it might produce.

Comparative Analysis of Regression Models for Chicken Carcass Volume Estimation Metrics

Table 13 compares the various regression models for their performance in estimating chicken carcass volume, focusing on their R^2 and RMSE values across the training, validation, and test sets. Fine Gaussian SVR and Rational Quadratic GPR displayed remarkable performance, with high R^2 and low RMSE scores across all datasets, respectively, indicating exceptional predictive power. This suggests that fine-grained models are well-suited for capturing complex features and variations specific to chicken carcass volume. The fine-tree model leads the regression tree model; however, it is crucial to consider the trade-off between the granularity and overfitting. Coarser models, such as coarse trees, have weaker performance owing to their inability to capture complex patterns, emphasizing the importance of carefully tuning model hyperparameters.

Among Support Vector Regressors (**SVRs**), Cubic and Quadratic SVRs perform well, indicating their ability to handle nonlinear relationships. However, Fine Gaussian SVR outperformed them, suggesting that finer granularity in SVRs is crucial. Boosted and bagged trees also performed well, indicating that ensemble methods

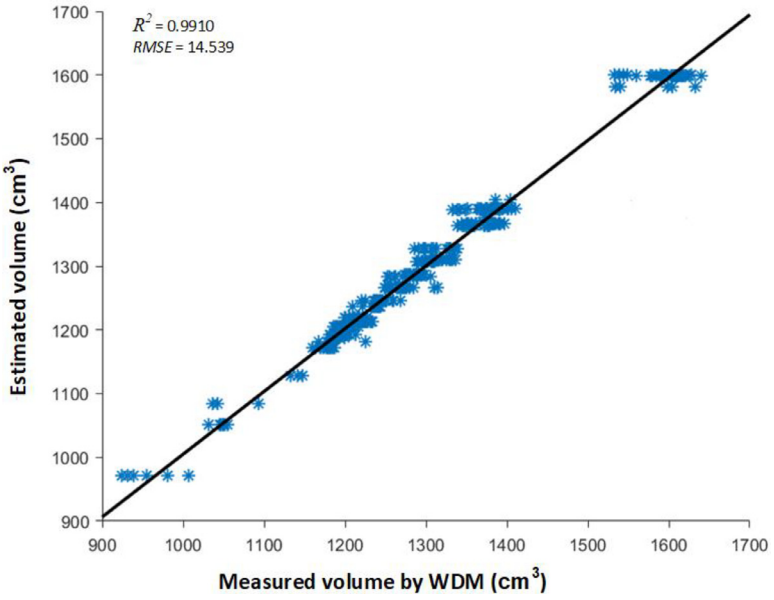

Figure 18. Scatter plot of the Bayesian regularization model.

Table 13. Comparative performance metrics ($\mathbf{R^2}$ and **RMSE**) of regression models across training, validation, and testing sets.

No.	Regression models	R^2			RMSE (cm^3)		
		Train	Validation	Testing	Train	Validation	Testing
1	Fine tree	0.9338	0.9053	0.9591	25.040	30.106	21.532
2	Medium tree	0.9023	0.8885	0.9289	30.798	34.445	24.056
3	Coarse tree	0.9017	0.8853	0.9059	31.813	37.928	29.189
4	Linear SVR	0.8726	0.8572	0.9088	35.787	46.902	28.773
5	Quadratic SVR	0.9082	0.9067	0.9119	38.176	41.666	23.426
6	Cubic SVR	0.9493	0.9346	0.9505	27.437	39.076	20.901
7	Fine Gaussian SVR	0.9852	0.9815	0.9928	18.291	22.862	12.978
8	Medium Gaussian SVR	0.9526	0.9417	0.9765	24.551	29.239	19.987
9	Coarse Gaussian SVR	0.8663	0.8598	0.8921	43.040	52.370	32.807
10	Rational quadratic GPR	0.9712	0.9639	0.9983	13.064	18.981	7.016
11	Squared exponential	0.9884	0.9863	0.9980	15.106	19.055	9.821
12	Matern 5/2 GPR	0.9938	0.9853	0.9982	14.022	18.236	8.475
13	Exponential GPR	0.9989	0.9947	0.9984	11.330	17.008	6.113
14	Least squares kernel	0.9572	0.9366	0.9639	27.757	29.045	24.044
15	SVR kernel	0.8858	0.8534	0.8925	48.551	50.485	45.457
16	Bagged trees	0.9902	0.9856	**0.9988**	7.480	8.843	**5.335**
17	Boosted trees	0.9650	0.9527	0.9733	14.874	17.624	10.001
18	Narrow neural network	0.9426	0.9217	0.9760	21.050	23.598	19.674
19	Wide neural network	0.9712	0.9639	0.9914	18.423	21.076	14.171
20	Medium neural network	0.9800	0.9751	0.9922	17.697	20.062	13.443
21	Bilayered neural network	0.9841	0.9703	0.9869	19.718	22.069	17.533
22	Trilayered neural network	0.9802	0.9794	0.9887	19.027	21.223	16.284
23	Levenberg-Marquardt ANN	0.9926	0.9802	0.9892	17.286	19.693	15.890
24	Bayesian regularization ANN	0.9922	0.9899	0.9910	16.937	17.328	14.539
25	Scaled conjugate gradient ANN	0.9093	0.8915	0.9199	38.459	46.475	27.296

Boldface shows the model with the highest R^2 and lowest RMSE values.

can provide accurate predictions in high-variability contexts such as carcass volume estimation. Within regression neural networks, performance varies, and more complex architectures such as trilayered neural networks do not necessarily outperform simpler ones. This raises questions about the application's "sweet spot" for model complexity. Bayesian Regularization stands out, but it does not uniformly outperform all metrics, raising concerns about its applicability to all aspects of the volume estimation task.

The results in Table 13 play a crucial role in our search for the most reliable model for estimating chicken carcass volume. The bagged tree model emerged as the best model, with an accuracy of 0.9988 and an RMSE value of only 5.335 cm^3 for the test set. A high accuracy value close to 1 indicates almost perfect predictive power, which means that the model estimates are highly reliable for applications requiring the highest accuracy, such as quality control in automated processing lines. Additionally, a low RMSE value indicates that the model estimates are likely to deviate slightly from the actual measurements, thereby reducing the risk of costly errors in the production environment.

However, balancing this exceptional performance with computational demands is crucial. Bagged tree models can be computationally intensive, particularly when handling large datasets, which can slow down real-time processing or increase the computational costs. For settings where computational efficiency is a priority, simpler models, such as fine or medium trees, still offer robust predictive power (with R^2 values above 0.9) but are likely quicker and less resource intensive. These insights help industry professionals weigh the pros and cons of model selection based on their operations' unique demands, whether they prioritize maximum accuracy or optimize speed and efficiency.

The ideal chicken carcass volume estimation model is likely to capture complex nonlinear relationships, while avoiding overfitting. Fine Gaussian SVR, Rational Quadratic GPR, and certain ensemble methods, such as Boosted Trees, have the most balanced performance profiles. However, model selection must be nuanced considering the specific challenges posed by the variability inherent in biological datasets, such as chicken carcass volumes.

Table 14 provides a more detailed performance analysis by examining the performance of the 25 regression models in estimating chicken carcass volume through three key metrics: Mean Absolute Error (MAE), Mean Square Error (MSE), and Average Relative Error (ARE). These metrics are essential for different applications, because a low MAE is necessary for applications that require high accuracy in absolute terms. By contrast, a low MSE is critical for applications that are sensitive to outliers. Conversely, ARE is essential when the relative size of the errors in relation to the actual values is crucial.

The Bagged Trees and Exponential GPR were the most robust models among those evaluated, with the lowest ARE and MSE, respectively. These models provide a well-balanced performance across all three metrics, and may be ideal for applications that require comprehensive accuracy. However, the SVR Kernel appears to be less suitable owing to its high ARE of 7.059%, which may not satisfy the precision requirements of applications that require relative estimation.

When examining the models by category, tree-based approaches, such as Bagged and Boosted Trees, tended to outperform simpler Fine, Medium, and Coarse Trees,

Table 14. Comparative evaluation of regression models using MAE, MSE, and ARE metrics.

No.	Regression models	MAE (cm^3)	MSE (cm^6)	ARE (%)
1	Fine tree	8.937	463.627	4.613
2	Medium tree	9.399	578.691	4.859
3	Coarse tree	10.987	851.997	5. 294
4	Linear SVR	10.752	827.885	4.973
5	Quadratic SVR	9.792	548.777	4.712
6	Cubic SVR	8.591	436.851	4.031
7	Fine Gaussian SVR	6.168	168.428	3.015
8	Medium Gaussian SVR	7.629	399.480	3.718
9	Coarse Gaussian SVR	11.594	1076.299	5.043
10	Rational quadratic GPR	6.027	49.224	3.036
11	Squared exponential	8.436	96.452	3.665
12	Matern 5/2 GPR	7.765	71.825	3.456
13	Exponential GPR	5.639	37.363	2.971
14	Least squares kernel	8.213	578.113	4.841
15	SVR kernel	20.639	2066.338	7.059
16	Bagged trees	**4.950**	**28.462**	**2.125**
17	Boosted trees	6.639	100.020	3.359
18	Narrow neural network	7.069	387.066	3.932
19	Wide neural network	6.783	200.817	3.402
20	Medium neural network	6.102	180.714	3.250
21	Bilayered neural network	6.982	307.406	3.634
22	Trilayered neural network	6.022	265.168	3.037
23	Levenberg-Marquardt ANN	6.908	252.492	3.019
24	Bayesian regularization ANN	6.772	211.382	2.975
25	Scaled conjugate gradient ANN	8.956	745.071	3.986

The boldface shows the model with the lowest MAE, MSE and ARE values.

particularly in terms of ARE. Similarly, advanced neural network architectures, such as Bilayered and Trilayered networks, perform better than simpler Neural Network models. These findings suggest that more complex algorithms provide more accurate predictions; however, this comes at the cost of an increased computational intensity and potential overfitting. Therefore, the choice between more straightforward and complex models depends on the requirements of the application, including an acceptable trade-off between the computational cost and predictive accuracy. These results can guide the selection of model categories for future research and applications, and multi-metric evaluation provides a comprehensive approach for selecting the most appropriate models for chicken carcass volume estimation, depending on specific accuracy requirements.

Processing Speed Evaluation for Volume Estimation With Bagged Trees

After assessing various regression models for mean absolute error (MAE), mean squared error (MSE), and absolute relative error (ARE), the bagged tree model was found to be the most accurate based on these metrics. To investigate the performance of the model further, its processing speed was evaluated using a dataset of 30 randomly selected chicken carcasses. The processing time, from initiating 3-D imaging to finalizing the volume estimation, was precisely measured using MATLAB software, and each carcass was evaluated three times to obtain the average processing time.

The choice of Bagged Trees as the primary machine learning algorithm was driven by its proven effectiveness in handling high-dimensional data and resistance to overfitting. Cross-validation techniques are employed during the training process to ensure the robustness and reliability of the model. Specifically, a k-fold cross-validation approach was used to validate the performance of the model and to provide an unbiased estimate of its generalizability. Additionally, hyperparameter tuning was conducted using a grid search to optimize key parameters such as the number of trees and the maximum depth of the trees. This process aims to balance the model complexity and predictive accuracy, minimizing the risk of overfitting while enhancing model performance. These steps are critical for refining the model and ensuring that it performs well on unseen data, thereby increasing its practical applicability in diverse operational settings.

The graph in Figure 19 shows that the computational speed of the bagged tree model remained consistent across different carcass volumes, with 30 empirically obtained data points demonstrating that the processing time remained consistently variable. Despite variables

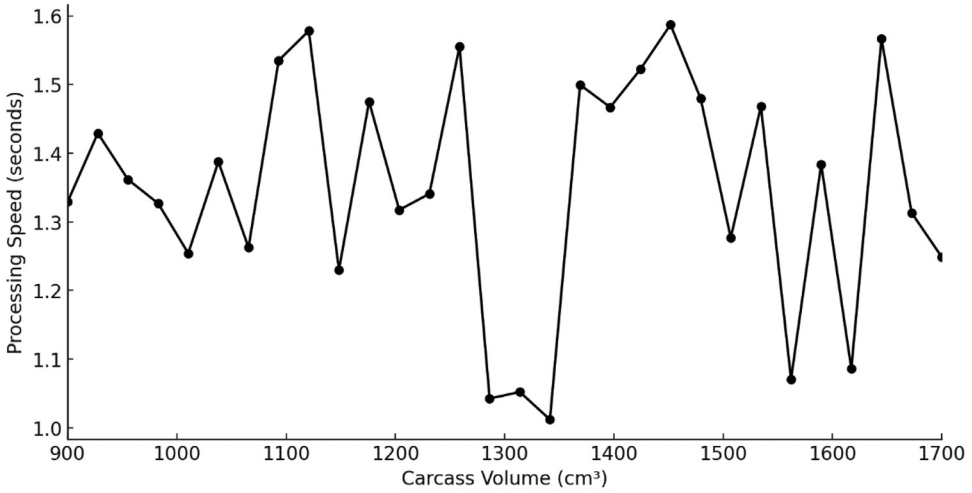

Figure 19. Line graph illustrating the correlation between carcass volume (cm^3) and the corresponding average processing time (seconds) when employing the bagged tree regression model for volume estimation.

Table 15. T-test comparison of measured vs. estimated volumes in bagged trees model ($\boldsymbol{P} < 0.05$).

No.	Regression model	Measured WDM vol (cm^3) *mean* ± *std*	Estimated vol (cm^3) *mean* ± *std*
1	Bagged trees	1,412.736 ± 182.634[a]	1,420.874 ± 191.456[a]

[a,b]Mean ± std within a row, with no superscript in common, differ significantly ($P < 0.05$)

such as mechanical vibrations and constant carcass movement at higher speeds, proper synchronization settings maintained an average processing speed of less than 1.6 s. Specifically, a processing time of approximately 1.3 s was observed for a 1600 cm^3 carcass and 1.5 s for a 1,200 cm^3 carcass, indicating that carcass size did not significantly affect processing speed. The statistical t-test analysis corroborated these findings, demonstrating that the observed differences were significant ($P < 0.05$) (Table 15).

The bagged tree model has high accuracy and rapid processing speed, making it an ideal choice for industrial applications. This speed could result in a 50% reduction in labor costs and an increase in operational efficiency. The t-test analysis presented in Table 15 compares the actual and estimated volumes in the bagged tree model, and the results confirm a statistical significance of $P < 0.05$. The mean measured volume was 1,412.736 cm^3 with a standard deviation of 182.634, while the estimated volume was marginally greater, with a mean of 1,420.874 cm^3 and a standard deviation of 191.456. The superscript 'a' appended to the standard deviations denotes that the differences between the paired means are not statistically significant, conforming to the $P <$ 0.05 significance level.

There are opportunities for future research to optimize the bagged tree model through algorithmic enhancements, such as feature reduction or parallel processing, which would further improve processing speed. In addition, comparing the processing speed of the bagged tree model with that of other state-of-the-art methods would provide a comprehensive understanding of its relative efficiency.

DISCUSSION

To our knowledge, this is the first study to estimate chicken volume using computer vision and machine learning technologies. This research is groundbreaking, as it introduces a novel automated approach that significantly enhances the accuracy and efficiency of carcass volume estimation. Traditional methods rely heavily on manual labor and 2-D imaging, which are prone to subjective errors and fail to capture the true volumetric characteristics of carcasses. By leveraging 3-D point cloud reconstruction and depth imaging, our method addresses these limitations and provides a more precise and reliable assessment. This advancement is crucial for the poultry industry, which requires high-throughput and accurate grading systems to optimize supply chain operations, reduce economic losses, and maintain product quality. The implementation of this technology could lead to more standardized grading processes, ultimately improving operational efficiency and industry standards.

Technological Advancements and Contributions

This study presents a significant advancement in the application of machine learning algorithms and 3-D imaging technologies to estimate chicken carcass volumes, offering a scalable alternative to conventional methodologies. By leveraging depth imaging and 3-D point cloud reconstruction, we achieved accurate and efficient volume estimation, surpassing traditional 2-D imaging and basic statistical techniques that mainly focus on weight assessments. Our results demonstrate that incorporating depth data enhances predictive model accuracy by capturing critical spatial details of carcass structure, thus achieving a higher level of computational precision.

A novel contribution of this study is the effective utilization of 3-D data, which significantly improves the performance of machine learning models. Notably, the bagged tree algorithm demonstrated proficiency in managing high-dimensional data and avoiding overfitting, making it suitable for handling complex 3-D data. However, the accuracy of the volume estimation is closely related to the quality of the initial surface mesh and granularity of the partitioning. Inaccuracies in these aspects can result in significant computational errors. Empirical evaluations revealed a variance of up to 5 to 10% in model accuracy when using low-quality meshes. The integration of depth data allowed for the capture of subtle variations in carcass shape and size, which are crucial for precise volume estimation. The empirical results showed high accuracy in volume estimation, with minimal computational error variance. The system's ability to operate in real-time on a production line demonstrates its practical applicability and potential for integration into existing poultry processing workflows.

Comparison With Traditional Methods

Traditional methods for estimating chicken carcass metrics primarily focus on weight through manual measurements or 2-D imaging techniques (Mortensen et al., 2016; Qi, et al., 2019; Nyalala et al., 2021b,c). Manual methods such as water displacement or physical measurements are labor-intensive and prone to human error, making them inefficient for high-throughput processing lines. Moreover, these methods are often subjective, leading to inconsistencies and variability in the results.2-D imaging techniques, which are more automated than manual methods, still suffer from significant limitations (Okinda, et al., 2019). They primarily capture surface-level information, failing to account for the complex three-dimensional shapes of chicken carcasses. Consequently, these methods can produce inaccurate

estimations owing to occlusions, perspective distortions, and manual handling errors.

In contrast, our approach leverages advanced computer vision and machine learning technologies to capture comprehensive 3-D data of chicken carcasses. By utilizing depth imaging and 3-D point cloud reconstruction, we can accurately model the entire carcass structure, overcoming the limitations of 2-D methods. This allows for a more precise and consistent estimation, reducing the errors associated with manual measurements and 2-D imaging. The bagged tree algorithm used in our study further enhances accuracy by effectively handling high-dimensional data and avoiding overfitting, which is a common issue in traditional statistical models. This machine learning approach enables the system to learn from a large dataset of carcass images, thereby improving its predictive accuracy over time. In addition, the integration of real-time data capture and processing capabilities ensures that our method is suitable for high-throughput industrial applications. This contrasts with the time-consuming nature of manual methods and limited scalability of 2-D imaging techniques. The ability to operate in real-time not only enhances operational efficiency but also supports better decision-making and quality control in poultry processing. In summary, our study demonstrates significant advantages over traditional estimation methods by providing a more accurate, consistent, and scalable solution. The use of 3-D imaging and machine learning technologies addresses the inherent limitations of manual and 2-D methods, offering a revolutionary approach to poultry carcass volume estimation.

Limitations and Future Directions

Despite the high accuracy achieved using our approach, several limitations must be acknowledged. First, the dependency on the quality of the initial surface mesh and the granularity of partitioning pose significant challenges. Inaccuracies in these areas can lead to substantial computational errors, as shown by empirical evaluations, indicating a variance of up to 5-10% in model accuracy with low-quality meshes. This underscores the necessity for high-resolution imaging and precise calibration to ensure a reliable volume estimation. Another critical limitation is the controlled environment of this study, which may not fully capture the variability encountered in commercial poultry processing plants. Variables, such as changes in lighting, carcass orientation, and sensor placement, have not been thoroughly investigated. To enhance the robustness of the model, future research should systematically examine these factors in diverse real-world scenarios. The computational demands of processing 3-D data in real-time are another significant constraint. The resource consumption of 3-D-based models is approximately 30% higher than 2-D models, potentially limiting their applicability in small-scale operations with restricted computational resources. Future work should prioritize the development of lightweight models or optimizing the computational pipeline to facilitate deployment on less powerful hardware, making the method accessible to a broader range of users.

To enhance the adaptability of the models, future studies should include additional features, such as curvature and texture metrics, which could improve predictive performance and generalizability. Moreover, exploring other machine learning models, such as Support Vector Machines (**SVMs**) or Neural Networks, under different environmental conditions and dataset characteristics will provide valuable insights into their stability and performance. Additionally, developing methods to integrate multispectral or hyperspectral imaging with 3-D point cloud data could provide more comprehensive assessments, including the detection of internal qualities and defects. This integration could significantly advance the capabilities of automated grading systems in the poultry industry. In summary, although the proposed method offers significant advancements in accuracy and efficiency, addressing these limitations through targeted future research will be crucial for further development and validation. This will ensure the reliability and scalability of the technology, paving the way for broader adoption in the poultry industry and potentially other sectors requiring precise volumetric assessments.

Broader Implications and Ethical Considerations

Having demonstrated the technical efficacy of our volume estimation models, we now consider their broader implications for the poultry industry, including potential impacts on labor and ethical considerations.

Although the proposed method offers significant technical and economic benefits such as improved accuracy in volume estimation and reduced labor costs, it is crucial to consider its ethical implications, particularly concerning labor displacement. The adoption of advanced automation technologies in the poultry industry may reduce the demand for manual labor, potentially impacting workers who rely on these jobs. To mitigate these negative effects, it is essential to implement measures such as upskilling and reskilling programs for affected workers. These programs can provide new opportunities for more technologically advanced roles, such as operating and maintaining automated systems, data analysis, and quality control. Furthermore, companies can collaborate with educational institutions and government agencies to facilitate the transition of workers into new employment areas, thus ensuring that the benefits of technological advancement are shared more equitably.

Ethical considerations should guide the implementation of these technologies. This includes maintaining transparency with employees regarding potential changes and impacts, offering fair compensation and support during transitions, and ensuring that automation does not compromise the quality of life and working

conditions of the remaining employees. As the poultry industry evolves, a balanced approach that considers both technological innovation and workforce welfare is essential.

The implications of this study extend beyond the poultry industry and offer potential applications in various sectors that require precise volumetric measurement. For instance, these methods can be adapted for sorting and grading fruits and vegetables, where the shape and size are critical quality indicators. In industrial manufacturing, similar technologies can improve the quality control processes, reduce waste, and increase operational efficiency. Future research directions include exploring the integration of multispectral or hyperspectral imaging with 3-D point cloud data to detect internal qualities and defects. Additionally, developing lightweight models optimized for edge computing could make this technology more accessible to smaller farms and operations. Transfer learning techniques can further enhance the flexibility of a system, allowing rapid adaptation to new tasks with minimal retraining.

This study provides a comprehensive foundation for the application of machine learning and 3-D imaging technologies in poultry management. The proposed method offers significant improvements over traditional techniques and has the potential for broader applicability in the agricultural sector. However, further validation and optimization are necessary to ensure the reliability and efficiency of this method across different operational contexts.

CONCLUSIONS

This study marks a notable advancement in poultry volume estimation technology through the integration of computer vision, 3-D imaging, and machine learning algorithms. Among the 25 evaluated techniques, the selection of the bagged tree model underscores its robustness and precision, which is attributed to its ensemble nature and its resistance to overfitting. Rigorous statistical validation, including t-tests, confirmed the computational efficiency of the model and the efficacy of incorporating selected 2-D and 3-D features. Despite the challenges of surface reconstruction quality and computational resource demands, the model demonstrated rapid processing capabilities, offering potential labor cost reductions of up to 50%, thereby presenting significant economic advantages. Our research not only introduces a comprehensive multidimensional approach but also positions itself as a pioneering contribution within both the scientific community and industrial applications. The low cost, robustness, and scalability of this methodology underscore its potential for widespread adoption, paving the way for further research and refinement. Future work should continue to enhance model adaptability and computational efficiency, address current limitations, and expand the scope of automated volume-estimation technologies in various sectors. This study lays a strong foundation for subsequent innovations, advocating for a more automated and precise approach in the poultry industry and other domains that require accurate volumetric assessments.

ACKNOWLEDGMENTS

This study was supported by the National Science and Technology Support Program (No.2015BAD19806) of the College of Engineering, Nanjing Agricultural University, China.

DISCLOSURES

The authors declare no conflicts of interest.

REFERENCES

Adamczak, L., M. Chmiel, T. Florowski, D. Pietrzak, M. Witkowski, and T. Barczak. 2018. The use of 3D scanning to determine the weight of the chicken breast. Comp. Electr. Agric. 155:394–399.

Bhargava, A., and A. Bansal. 2021. Fruits and vegetables quality evaluation using computer vision: a review. J. King Saud Univ.-Comp. Inform. Sci. 33:243–257.

Bishop, C. M., and N. M. Nasrabadi. 2006. Pattern Recognition and Machine Learning. Springer, New York, NY.

Burden, F., and D. Winkler. 2009. Bayesian regularization of neural networks. Pages 23−42 in Artificial Neural Networks: Methods and Applications. Humana, Totowa, NJ.

Canny, J. 1986. A computational approach to edge detection. IEEE Trans. Pattern Anal. Mach. Intell. 8:679–698.

Chai, T., and R. R. Draxler. 2014. Root mean square error (RMSE) or mean absolute error (MAE)?−arguments against avoiding RMSE in the literature. Geosci. Model Develop. 7:1247–1250.

Chalidabhongse, T., P. Yimyam, and P. Sirisomboon. 2006. 2D/3D vision-based mango's feature extraction and sorting.

Chan, T. F., and L. A. Vese. 2001. Active contours without edges. IEEE Transact. Image Proc. 10:266–277.

Chicco, D., M. J. Warrens, and G. Jurman. 2021. The coefficient of determination R-squared is more informative than SMAPE, MAE, MAPE, MSE and RMSE in regression analysis evaluation. PeerJ Comp. Sci. 7:e623.

Concha-Meyer, A., J. Eifert, H. Wang, and G. Sanglay. 2018. Volume estimation of strawberries, mushrooms, and tomatoes with a machine vision system. Int. J. Food Prop. 21:1867–1874.

Di Bucchianico, A. 2008. Coefficient of determination (R 2). Encyclopedia of statistics in quality and reliability.

E Woods, R., and R. C Gonzalez. 2008. Digital image processingPearson Education Ltd.

Gavin, H. P. 2019. The Levenberg-Marquardt Algorithm for Nonlinear Least Squares Curve-Fitting Problems. Department of Civil and Environmental Engineering. (p. 19). Duke University, Durham, NC, USA, 19.

Hartley, R., and A. Zisserman. 2003. Multiple View Geometry in Computer Vision. Cambridge University Press, England.

Holz, D., A. E. Ichim, F. Tombari, R. B. Rusu, and S. Behnke. 2015. Registration with the point cloud library: a modular framework for aligning in 3-D. IEEE Robotics Auto. Mag. 22:110–124.

Hsu, H., and P. A. Lachenbruch. 2014. Paired t test. Wiley StatsRef: statistics reference online.

Huang, Q., J. Mao, and Y. Liu. 2021. An improved grid search algorithm of SVR parameters optimization.

Huang, Y., L. J. Kangas, and B. A. Rasco. 2007. Applications of artificial neural networks (ANNs) in food science. Crit Rev Food Sci Nutr 47:113–126.

Jacobson, N. 2013. Lectures in Abstract Algebra: II. Linear Algebra. Springer Science & Business Media, New York.

James, G., D. Witten, T. Hastie, and R. Tibshirani. 2013. An Introduction to Statistical Learning. Springer, New York.

Jørgensen, A., J. V. Dueholm, J. Fagertun, and T. B. Moeslund. 2019 Weight estimation of broilers in images using 3D prior knowledge.

Korohou, T., C. Okinda, H. Li, Y. Cao, I. Nyalala, L. Huo, M. Potcho, X. Li, and Q. Ding. 2020. Wheat grain yield estimation based on image morphological properties and wheat biomass. Journal of Sensors 2020:1571936.

Kuhn, M., and K. Johnson. 2013. Applied Predictive Modeling. Springer, New York.

Kurillo, G., E. Hemingway, M.-L. Cheng, and L. Cheng. 2022. Evaluating the accuracy of the azure kinect and kinect v2. Sensors 22:2469.

Labute, P. 2008. The generalized Born/volume integral implicit solvent model: estimation of the free energy of hydration using London dispersion instead of atomic surface area. J Comput Chem 29:1693–1698.

Lachat, E., H. Macher, T. Landes, and P. Grussenmeyer. 2015. Assessment and calibration of a RGB-D camera (Kinect v2 Sensor) towards a potential use for close-range 3D modeling. Remote Sensing 7:13070–13097.

Loh, W. Y. 2011. Classification and regression trees. Wiley Interdis. Rev.: Data Mining Knowl. Disc. 1:14–23.

Luo, Y., Z. Mi, and W. Tao. 2021 Deepdt: Learning geometry from delaunay triangulation for surface reconstruction.

Mortensen, A. K., P. Lisouski, and P. Ahrendt. 2016. Weight prediction of broiler chickens using 3D computer vision. Comp. Electr. Agric. 123:319–326.

Nyalala, I., C. Okinda, Q. Chao, P. Mecha, T. Korohou, Z. Yi, S. Nyalala, Z. Jiayu, L. Chao, and C. Kunjie. 2021a. Weight and volume estimation of single and occluded tomatoes using machine vision. Int. J. Food Prop. 24:818–832.

Nyalala, I., C. Okinda, C. Kunjie, T. Korohou, L. Nyalala, and Q. Chao. 2021b. Weight and volume estimation of poultry and products based on computer vision systems: a review. Poult. Sci. 100:101072.

Nyalala, I., C. Okinda, N. Makange, T. Korohou, Q. Chao, L. Nyalala, Z. Jiayu, Z. Yi, K. Yousaf, L. Chao, and C. Kunjie. 2021c. On-line weight estimation of broiler carcass and cuts by a computer vision system. Poult. Sci. 100:101474.

Nyalala, I., C. Okinda, L. Nyalala, N. Makange, Q. Chao, L. Chao, K. Yousaf, and K. Chen. 2019. Tomato volume and mass estimation using computer vision and machine learning algorithms: cherry tomato model. J. Food Eng. 263:288–298.

Okinda, C., M. Lu, L. Liu, I. Nyalala, C. Muneri, J. Wang, H. Zhang, and M. Shen. 2019. A machine vision system for early detection and prediction of sick birds: a broiler chicken model. Biosyst. Eng. 188:229–242.

Okinda, C., M. Lu, I. Nyalala, J. Li, and M. Shen. 2018. Asphyxia occurrence detection in sows during the farrowing phase by inter-birth interval evaluation. Comp. Electr. Agric. 152:221–232.

Okinda, C., I. Nyalala, T. Korohou, C. Okinda, J. Wang, T. Achieng, P. Wamalwa, T. Mang, and M. Shen. 2020a. A review on computer vision systems in monitoring of poultry: a welfare perspective. Artif. Intell. Agric. 4:184–208.

Okinda, C., Y. Sun, I. Nyalala, T. Korohou, S. Opiyo, J. Wang, and M. Shen. 2020b. Egg volume estimation based on image processing and computer vision. J. Food Eng. 283:110041.

Oviedo-Rondon, E. O., J. Parker, and S. Clemente-Hernandez. 2007. Application of real-time ultrasound technology to estimate in vivo breast muscle weight of broiler chickens. Br. Poult. Sci. 48:154–161.

Pagliari, D., and L. Pinto. 2015. Calibration of kinect for xbox one and comparison between the two generations of microsoft sensors. Sensors 15:27569–27589.

Penning, B. W., W. M. Snelling, and M. J. Woodward-Greene. 2020. Machine learning in the assessment of meat quality. IT Professional 22:39–41.

Petrou, M. M. P., and C. Petrou. 2010. Image Processing: The Fundamentals. John Wiley & Sons, Hoboken, New Jersey, U.S.

Qi, C., J.-q. Xu, C. Liu, M.-q. Wu, and K.-j. Chen. 2019. Automatic classification of chicken carcass weight based on machine vision and machine learning technology.

Quinonero-Candela, J., C. E. Rasmussen, and C. K. I. Williams. 2007. Approximation methods for Gaussian process regression. Pages 203−223 in Large-Scale Kernel Machines. MIT Press, Cambridge, Massachusetts, USA.

Sahu, S., H. Sarma, and D. J. Bora. 2018 Image segmentation and its different techniques: An in-depth analysis.

Said, K. A. M., A. B. Jambek, and N. Sulaiman. 2016. A study of image processing using morphological opening and closing processes. Int. J. Cntrl Theory Appl. 9:15–21.

Samarasinghe, S. 2016. Neural Networks for Applied Sciences and Engineering: From Fundamentals to Complex Pattern Recognition. CRC Press, Boca Raton, Florida, USA.

Schulz, E., M. Speekenbrink, and A. Krause. 2018. A tutorial on Gaussian process regression: modelling, exploring, and exploiting functions. J Mathem. Psychol. 85:1–16.

Scollan, D., N. L. J. Caston, Z. Liu, A. K. Zubair, S. Leeson, and B. W. McBride. 1998. Nuclear magnetic resonance imaging as a tool to estimate the mass of the pectoralis muscle of chickens in vivo. Br. Poult. Sci. 39:221–224.

Shahbandeh, M. 2023. Global per capita meat consumption 2022-2032. Hamburg, Germany. https://www.statista.com/statistics/739920/.

Sutton, C. D. 2005. Classification and regression trees, bagging, and boosting. Handbook of Statistics 24:303–329.

Szeliski, R. 2022. Computer Vision: Algorithms and Applications. Springer Nature, Seatlle, WA, USA.

Wasenmüller, O., and D. Stricker. 2017 Comparison of kinect v1 and v2 depth images in terms of accuracy and precision.

Williams, C. K. I., and C. E. Rasmussen. 2006. Gaussian processes for machine learning. MIT press, Cambridge, MA.

Yang, L., L. Zhang, H. Dong, A. Alelaiwi, and A. El Saddik. 2015. Evaluating and improving the depth accuracy of Kinect for Windows v2. IEEE Sensors J 15:4275–4285.